Massive MIMO Downlink for Wireless Information and Energy Transfer With Energy Harvesting Receivers

Long Zhao, *Member, IEEE*, and Xiaodong Wang, *Fellow, IEEE*

***Abstract*—We consider a system where a massive multiple-input multiple-output (MIMO) base station (BS) transmits information and energy to multiple energy harvesting receivers. Each receiver has no power source and needs to harvest sufficient energy in order to decode its message from the received signal. Under either the power splitting mode or the time switching mode at the receivers, we consider two design problems. One is to maximize the minimum transmission rate among all receivers and the other is to optimize the system energy efficiency (EE) through jointly designing the power allocation proportions at the BS and the power splitting (or time switching) factors at the receivers. The optimal solutions to these problems are obtained either in terms of closed-form expressions or efficient algorithms by leveraging the asymptotic channel orthogonality and hardening effects of massive MIMO. The simulation results indicate that the power splitting mode outperforms the time switching mode in terms of both the minimum transmission rate and the system EE.**

***Index Terms*—Wireless information and energy transfer, massive MIMO, circuit energy consumption, transmission rate, energy efficiency.**

I. Introduction

WIRELESS energy transfer has been recognized as a promising technique to cut the last mile limiting the "true wireless" communications [1], [2]. It can empower the terminals by radio-frequency (RF) signal transmission or near-field coupling through inductive coils [3], [4]. Together with wireless information transmission, wireless information and energy transfer has been extensively studied in recent years [5]–[7]. When a base station (BS) transmits RF signal to the single-antenna receivers, each receiver can decode information and harvest energy taking advantage of frequency division, power splitting (PS) or time switching (TS) modes [4], [8]. Considering the scarcity of frequency resources, PS and TS modes are considered practically more feasible.

Manuscript received June 16, 2018; revised October 10, 2018 and December 1, 2018; accepted January 19, 2019. Date of publication January 29, 2019; date of current version May 15, 2019. This work was supported by the China Natural Science Funding under Grant 61601044, and by the Leading Talents Program of Guangdong Province under grant 00201510, and the Shenzhen Peacock Program under grant KQTD2015071715073798. The associate editor coordinating the review of this paper and approving it for publication was R. Zhang. *(Corresponding author: Xiaodong Wang.)*

L. Zhao is with the Key Laboratory of Universal Wireless Communications, Ministry of Education, Beijing University of Posts and Telecommunications, Beijing 100876, China (e-mail: z-long@bupt.edu.cn).

X. Wang is with the Electrical Engineering Department, Columbia University, New York, NY 10027 USA (e-mail: wangx@ee.columbia.edu).

Color versions of one or more of the figures in this paper are available online at http://ieeexplore.ieee.org.

Digital Object Identifier 10.1109/TCOMM.2019.2895868

The massive multiple-input multiple-output (MIMO) technique can focus the received signal power with extremely narrow beams [9], [10] and therefore has been considered in wireless information and energy transfer systems [11], [12]. The feasibility of wireless energy transfer with massive MIMO has been studied for sensor networks and the outage probability of energy harvesting was analyzed [13]. Exploiting the power superposition of multi-cell massive MIMO systems, a cooperative energy transfer scheme was proposed in order to enhance the energy transfer efficiency for multiple receivers in multi-cell scenarios [12]. Based on [12], a retrodirective energy transfer technique with massive MIMO is proposed for multiple receivers in [14]. Moreover, considering the uplink information transmission of multiple receivers powered by downlink energy transfer with massive MIMO, the uplink transmission rate was investigated for different detectors [11].

A. Motivation

In the existing literature, the harvested energy at receivers is mainly used to charge their batteries for future usage [8], [12] or to supply the radiated power of power amplifiers (PAs) for information transmission [15]–[17]. Recently, the harvested energy has been considered for the receiver circuit power consumption [18], [19]. Specifically, taking into account a constant circuit power consumption, an on-off power splitting scheme is proposed in order to improve the outage performance of the power splitting receiver [18]. Assuming that the power consumption of channel decoding is a convex function of the gap to channel capacity, harvest-then-receive and harvest-when-receive modes are studied to maximize the transmission rate of the time-switching receiver [19]. However, only one simple power consumption model for binary symmetric channel was given and the performance of power splitting receiver was not considered. Moreover, in general the circuit power consumption consists of both the constant power term and the rate-dependent power term for a practical receiver [20].

On the other hand, the objectives of wireless information and energy transfer mainly focus on maximizing the harvested energy while guaranteeing the transmission rate requirements [12], or maximizing the uplink transmission rates of the users powered by the downlink energy transfer [11], or reducing the outage probability of harvested energy at receivers [13]. On the other hand, the energy efficiency (EE) is another important system performance metric. The round-trip EE has been studied for massive MIMO systems when the uplink information transmission is powered by downlink energy transfer [21], [22]. However, the harvested energy used to power the uplink transmission and the circuit power consumption is assumed to be from batteries [21], [22]. Therefore, the EE maximization for downlink information and energy transfer is an open research problem when the harvested energy is used for message decoding at the receivers.

B. Contributions

This paper considers a downlink massive MIMO system that employs matched-filtering (MF) beamformers to simultaneously serve multiple energy harvesting receivers. Each receiver employs the power splitting or time switching mode to harvest energy from the received signal in order to power its information decoding circuit. By jointly optimizing the power allocation proportions at the BS and power splitting (or time switching) factors at the receivers, one aim is to maximize the minimum transmission rate of all receivers in order to guarantee the fairness; another is to optimize the system EE in order to improve the power efficiency. The solutions to these formulated problems are obtained either in terms of closed-form expressions or efficient algorithms. Results indicate that the power splitting mode outperforms the time switching mode in terms of both the minimum transmission rate and the system EE.

Our contributions in this paper are three-fold:

- We consider the practical scenario that the harvested energy of receivers is used to support the power consumption of information decoding circuits, which received less attention in the existing literature. Especially, the power consumption of information decoding circuits contains both the rate-dependent term and the constant term, which makes both the max-min transmission rate and system EE optimization problems challenging. Moreover, the channel estimation accuracy is also taken into account for the formulated problems.
- For the max-min transmission rate problem, the power allocation proportions and the power splitting (or time switching) factors jointly determine the harvested energy and transmission rate. On the other hand, the harvested energy of each receiver should meet the requirement of information decoding circuit, which results in that a transcendental equation needs to be solved in the formulated problem. Therefore, the closed-form solution was derived for the power splitting mode by leveraging the Lambert function; and a heuristic algorithm is proposed for the time switching mode.
- The EE optimization problems for both the power splitting and time switching modes are formulated and studied in the considered scenario. The adopted power consumption model at the BS contains both the transmit power and circuit power. By transforming the formulated problems into convex forms, two efficient algorithms are proposed to optimize the system EE while satisfying the transmission rate requirements. Finally, the EE comparison of the power splitting and time switching modes is given for the downlink information and energy transfer in details.

The remainder of this paper is organized as follows. Section II describes the system model and formulates the max-min transmission rate problem and EE optimization problem. Sections III and IV develop the optimal solutions to the formulated problems under power splitting and time switching modes, respectively. Simulation results are given in Section V and finally, Section VI contains the conclusions.

II. System Model and Problem Formulation

A. System Model

We consider a wireless information and energy transfer system with bandwidth B, where one BS employing M antennas simultaneously serves $K\ (\ll M)$ single-antenna receivers, labeled as $\mathcal{K} = \{1, 2, \cdots, K\}$. The system operates in a time-division duplex (TDD) mode and by channel reciprocity, the downlink channels can be obtained through uplink pilot transmission. As illustrated in Fig. 1, the receivers adopt the power splitting (Fig. 1(a)) or time switching (Fig. 1(b)) mode to harvest energy from a portion of their received signals. The harvested energy of each receiver should meet the power consumption of the signal processing circuit for information decoding. Moreover, the linear energy harvesting model [11]–[13] at the receivers is assumed and the uplink pilot and information transmission is ignored without considering different implementation-specific aspects. Another, the asymptotic channel orthogonality and hardening effects [9], [12], [14], [23] are employed in order to show the asymptotically theoretical performance and simplify the analysis in the considered system.

1) Channel Model: Block fading channels are assumed so that channels remain constant within a coherence time interval T and may change between blocks. Denote $\mathbf{g}_k^{\mathrm{H}} = \delta_k^{1/2}\mathbf{h}_k^{\mathrm{H}} \in \mathbb{C}^{1\times M}$ as the channel vector from the BS to the $k\mathrm{th}$ receiver, where δ_k is the large-scale fading coefficient that incorporates path loss and shadowing effect, and $\mathbf{h}_k = [h_{k1}, h_{k2}, \cdots, h_{kM}]^{\mathrm{T}}$ contains the fast fading coefficients, which are independent and identically distributed (i.i.d.) complex Gaussian random variables with zero mean and unit variance. Moreover, considering the minimum mean-square error or MF channel estimation at the BS, we assume that

$$\mathbf{h}_k = \sqrt{\theta_k}\hat{\mathbf{h}}_k + \sqrt{1-\theta_k}\boldsymbol{\varepsilon}_k, \quad k \in \mathcal{K}, \tag{1}$$

where the estimate $\hat{\mathbf{h}}_k \sim \mathbb{CN}(\mathbf{0}, \mathbf{I}_M)$ is independent of the error $\boldsymbol{\varepsilon}_k \sim \mathbb{CN}(\mathbf{0}, \mathbf{I}_M)$ of $\mathbf{h}_k$, and $\theta_k \in [0, 1]$ determines the estimation accuracy [12], [13], [24], [25].

2) Downlink Signal Transmission: The low-complexity MF is an asymptotically optimal information beamformer and an optimal energy beamformer in massive MIMO systems [9], [11], [12], therefore is employed at the BS in this paper.

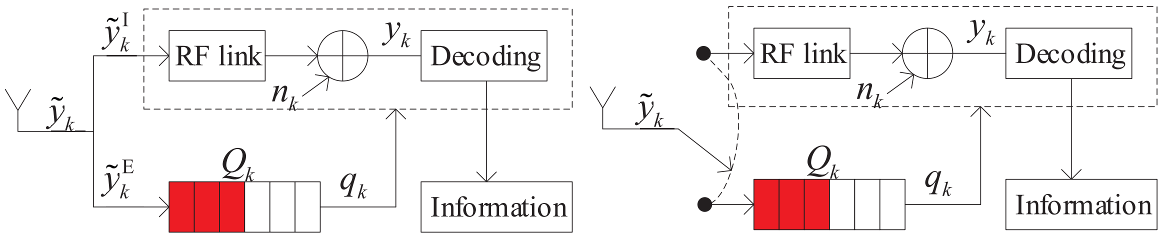

(a) Power splitting receiver. (b) Time switching receiver.

Fig. 1. Illustration of energy harvesting receivers.

Based on the estimated channels, the MF beamformer of the $k\mathrm{th}$ receiver can be written as

$$\mathbf{w}_k = \hat{\mathbf{h}}_k \Big/ \left\| \hat{\mathbf{h}}_k \right\|, \quad k \in \mathcal{K}. \tag{2}$$

Assuming that $p = E/M$ is the total transmit power of the BS, where E is a constant, and $s_k \in \mathbb{C}$ with $\mathbb{E}[|s_k|^2] = 1$ represents the information symbol for the $k\mathrm{th}$ receiver, the received RF signal of the $k\mathrm{th}$ receiver is given by

$$\tilde{y}_k(\boldsymbol{\alpha}) = \mathbf{g}_k^{\mathrm{H}} \sum_{i=1}^{K} \sqrt{\alpha_i p}\, \mathbf{w}_i s_i + \tilde{n}_{\mathrm{A}k}, \tag{3}$$

where $\boldsymbol{\alpha} = [\alpha_1, \alpha_2, \cdots, \alpha_K]^{\mathrm{T}}$ with $\alpha_k > 0$ $(k \in \mathcal{K})$ contains the power allocation proportions satisfying $\mathbf{1}^{\mathrm{T}}\boldsymbol{\alpha} = 1$, and $\tilde{n}_{\mathrm{A}k} \sim \mathbb{CN}\left(0, \sigma_{\mathrm{A}k}^2\right)$ denotes the complex additive white Gaussian noise (AWGN) at the receive antenna of the $k\mathrm{th}$ receiver in the RF domain.

3) Harvested Energy and Information Rate: Substituting $\mathbf{g}_k^{\mathrm{H}} = \delta_k^{1/2}\mathbf{h}_k^{\mathrm{H}}$ and (1) into (3) as well as taking advantage of $\mathbb{E}[|\boldsymbol{\varepsilon}_k^{\mathrm{H}}\mathbf{w}_i|^2] = 1$, $\mathbf{1}^{\mathrm{T}}\boldsymbol{\alpha} = 1$ and $p = E/M$, the power of the received RF signal at the $k\mathrm{th}$ receiver is given by

$$\begin{aligned} |\tilde{y}_k(\boldsymbol{\alpha})|^2 &= p\delta_k \left\{ \theta_k \sum_{i=1}^{K} \alpha_i \left| \hat{\mathbf{h}}_k^{\mathrm{H}} \mathbf{w}_i \right|^2 \right. \\ &\quad \left. + (1-\theta_k) \sum_{i=1}^{K} \alpha_i \mathbb{E}\left[\left| \boldsymbol{\varepsilon}_k^{\mathrm{H}} \mathbf{w}_i \right|^2 \right] \right\} + \sigma_{\mathrm{A}k}^2 \\ &= \frac{E\delta_k}{M} \left(\theta_k \sum_{i=1}^{K} \alpha_i \left| \hat{\mathbf{h}}_k^{\mathrm{H}} \mathbf{w}_i \right|^2 + 1 - \theta_k \right) + \sigma_{\mathrm{A}k}^2. \end{aligned} \tag{4}$$

Substituting (2) into (4), and using $\hat{\mathbf{h}}_k^{\mathrm{H}}\hat{\mathbf{h}}_k/M \to 1$ and $\hat{\mathbf{h}}_k^{\mathrm{H}}\hat{\mathbf{h}}_i/M \to 0$ $(k \neq i)$ for large M [9], [12], [23], we obtain

$$|\tilde{y}_k(\boldsymbol{\alpha})|^2 \approx \alpha_k E \theta_k \delta_k + \sigma_{\mathrm{A}k}^2. \tag{5}$$

Denote $\beta_k \in [0,1]$ as the power splitting or time switching factor during a coherence time interval T, i.e., a proportion β_k of $|\tilde{y}_k(\boldsymbol{\alpha})|^2$ during the interval $(0,T)$ is harvested under the power splitting mode, or the whole power $|\tilde{y}_k(\boldsymbol{\alpha})|^2$ within the interval $(0, \beta_k T)$ is harvested under the time switching mode. Further, supposing that the power of the ambient noise is negligible compared with the power of received signal and the linear energy harvesting model is employed [7], [11], [13], the harvested power at the $k\mathrm{th}$ receiver can be written as

$$\begin{aligned} Q_k(\boldsymbol{\alpha}, \beta_k) &= \xi_k \beta_k |\tilde{y}_k(\boldsymbol{\alpha})|^2 & (6) \\ &\approx \xi_k \beta_k \alpha_k E \theta_k \delta_k, & (7) \end{aligned}$$

where $\xi_k \in [0,1]$ denotes the energy conversion efficiency that depends on the energy harvesting circuit at the $k\mathrm{th}$ receiver [13].

On the other hand, the remaining RF signal for information decoding can be expressed as

$$\tilde{y}_k^{\mathrm{I}}(\boldsymbol{\alpha}, \beta_k) = \begin{cases} \sqrt{1-\beta_k}\,\tilde{y}_k(\boldsymbol{\alpha}), & 0 \le t \le T \text{ for PS}, \\ \tilde{y}_k(\boldsymbol{\alpha}), & \beta_k T \le t \le T \text{ for TS}. \end{cases} \tag{8}$$

Transforming $\tilde{y}_k^{\mathrm{I}}(\boldsymbol{\alpha}, \beta_k)$ into a baseband signal, we have

$$y_k(\boldsymbol{\alpha}, \beta_k) = \begin{cases} \sqrt{1-\beta_k}\left(\mathbf{g}_k^{\mathrm{H}} \sum_{i=1}^{K} \sqrt{\alpha_i p}\, \mathbf{w}_i s_i + n_{\mathrm{A}k} \right) + n_k, \\ \quad 0 \le t \le T \text{ for PS}, \\ \mathbf{g}_k^{\mathrm{H}} \sum_{i=1}^{K} \sqrt{\alpha_i p}\, \mathbf{w}_i s_i + n_{\mathrm{A}k} + n_k, \\ \quad \beta_k T \le t \le T \text{ for TS}, \end{cases} \tag{9}$$

where $n_{\mathrm{A}k} \sim \mathbb{CN}\left(0, \sigma_{\mathrm{A}k}^2\right)$ is the equivalent baseband version of the passband noise $\tilde{n}_{\mathrm{A}k}$ and $n_k \sim \mathbb{CN}\left(0, \sigma_k^2\right)$ denotes the noise induced by circuit processing on the digital baseband signal.

The antenna noise $n_{\mathrm{A}k}$ can be ignored compared with the circuit processing noise n_k since $\sigma_{\mathrm{A}k}^2 \ll \sigma_k^2$ [26]. Therefore, substituting $\mathbf{g}_k^{\mathrm{H}} = \delta_k^{1/2}\mathbf{h}_k^{\mathrm{H}}$, $p = E/M$ and (1) into (9), the signal-to-interference-plus-noise ratio (SINR) of the $k\mathrm{th}$ receiver can be written as (10) at the top of the next page. Following the same line as in the derivation of (5), for large M, the SINR and transmission rate of the $k\mathrm{th}$ receiver are given respectively by

$$\rho_k(\alpha_k, \beta_k) = \begin{cases} (1-\beta_k)\dfrac{\alpha_k \theta_k E \delta_k}{\sigma_k^2}, & 0 \le t \le T \text{ for PS}, \\ \dfrac{\alpha_k \theta_k E \delta_k}{\sigma_k^2}, & \beta_k T \le t \le T \text{ for TS}, \end{cases} \tag{11}$$

$$\rho_k(\boldsymbol{\alpha},\beta_k)=\begin{cases}\dfrac{\alpha_k\theta_k\left|\hat{\mathbf{h}}_k^{\mathrm{H}}\mathbf{w}_k\right|^2}{\theta_k\sum\limits_{i=1,\neq k}^{K}\alpha_i\left|\hat{\mathbf{h}}_k^{\mathrm{H}}\mathbf{w}_i\right|^2+(1-\theta_k)\sum\limits_{i=1}^{K}\alpha_i\mathbb{E}\left[\left|\boldsymbol{\varepsilon}_k^{\mathrm{H}}\mathbf{w}_i\right|^2\right]+\dfrac{M\sigma_k^2}{E\delta_k(1-\beta_k)}}, & 0\le t\le T \text{ for PS},\\ \dfrac{\alpha_k\theta_k\left|\hat{\mathbf{h}}_k^{\mathrm{H}}\mathbf{w}_k\right|^2}{\theta_k\sum\limits_{i=1,\neq k}^{K}\alpha_i\left|\hat{\mathbf{h}}_k^{\mathrm{H}}\mathbf{w}_i\right|^2+(1-\theta_k)\sum\limits_{i=1}^{K}\alpha_i\mathbb{E}\left[\left|\boldsymbol{\varepsilon}_k^{\mathrm{H}}\mathbf{w}_i\right|^2\right]+\dfrac{M\sigma_k^2}{E\delta_k}}, & \beta_k T\le t\le T \text{ for TS}.\end{cases} \tag{10}$$

and

$$r_k(\alpha_k,\beta_k)=\begin{cases}B\log_2\left[1+\rho_k(\alpha_k,\beta_k)\right], & \text{for PS},\\ (1-\beta_k)B\log_2\left[1+\rho_k(\alpha_k,\beta_k)\right], & \text{for TS}.\end{cases} \tag{12}$$

4) Power Consumption Model and Energy Efficiency: Based on [20] and [27]–[30], a realistic power consumption model of the BS contains both the transmit power, p, consumed by PAs and the circuit power, $p_{\mathrm{C}}(\mathbf{r})$, consumed by signal processing. Therefore, the total power consumption of the BS is given by

$$p_{\mathrm{T}}(p,\mathbf{r})=\frac{p}{\varsigma}+p_{\mathrm{C}}(\mathbf{r}), \tag{13}$$

where ς represents the efficiency of PAs and the transmission rate vector $\mathbf{r}=[r_1,r_2,\cdots,r_K]^{\mathrm{T}}$. The circuit power consumption mainly consists of the following terms: the power for channel coding and modulation mapping $a\sum_{k=1}^{K}r_k$, where a denotes the average power consumption coefficient (PCC) of coding and modulation per bit; the power for computing the MF beamformer matrix $b_1MK+b_2K\approx b_1MK$, where b_1 and b_2 represent the average PCCs of complex multiplication and addition operations, respectively; the power of the active RF links b_0M, where b_0 means the average PCC of each RF link, including D/A converter, filter, up-conversion, etc.; and the fixed power consumption c, which is required for BS-cooling, control signaling, and load-independent power of baseband processors, etc. [20], [31]–[33]. Therefore, the circuit power consumption is a function of the transmission rate, the number of antennas, and the number of receivers, and can be written as

$$p_{\mathrm{C}}(\mathbf{r})=a\sum_{k=1}^{K}r_k+M(b_0+b_1K)+c. \tag{14}$$

At the kth receiver, as illustrated in Fig. 1(a) or 1(b), the circuit power consumption mainly consists of the following terms: the power of a single RF chain v_{k1}, where v_{k1} means the average power consumption of down-conversion, filter, A/D converter, etc.; the power for information demodulation and decoding u_kr_k, where u_k denotes the average PCC of demodulation and decoding per bit; and the fixed power consumption v_{k2}, which is required for receiver-cooling, control signaling, and load-independent power of baseband processors, etc. [20], [31]–[33]. Therefore, denoting $v_k=v_{k1}+v_{k2}$, the circuit power consumption of the kth receiver can be expressed as

$$q_k(r_k)=u_kr_k+v_k. \tag{15}$$

As the harvested power of the kth receiver in (7) should be larger than its circuit power consumption in (15), we require $q_k(r_k)\le Q_k(\alpha_k,\beta_k)$.

Considering the metric bit/Joule, the system EE is defined as the total transmission rate divided by the power consumption of the BS, i.e.,

$$\eta_{\mathrm{EE}}(p,\boldsymbol{\alpha},\boldsymbol{\beta})=\frac{\sum_{k=1}^{K}r_k(\alpha_k,\beta_k)}{p_{\mathrm{T}}(p,\mathbf{r})}. \tag{16}$$

B. Problem Formulations

Given the total transmit power p at the BS, one objective of this paper is to maximize the minimum transmission rate of all receivers while guaranteeing that the circuit power consumption of each receiver is met by its harvested power, i.e.,

$$\max_{\boldsymbol{\alpha},\boldsymbol{\beta}}\min_{k}\ \{r_k(\alpha_k,\beta_k)\} \tag{17}$$

$$\text{s.t. } \mathbf{1}^{\mathrm{T}}\boldsymbol{\alpha}=1, \tag{18}$$

$$0\le\beta_k\le1, \tag{19}$$

$$q_k(r_k)\le Q_k(\alpha_k,\beta_k),\quad k\in\mathcal{K}. \tag{20}$$

By adjusting the transmit power p, another objective of this paper is to optimize the EE while guaranteeing the transmission rate requirements $\bar{\mathbf{r}}=[\bar{r}_1,\bar{r}_2,\cdots,\bar{r}_K]^{\mathrm{T}}$ of all receivers, i.e.,

$$\max_{p,\boldsymbol{\alpha},\boldsymbol{\beta}}\ \eta_{\mathrm{EE}}(p,\boldsymbol{\alpha},\boldsymbol{\beta}) \tag{21}$$

$$\text{s.t. } \mathbf{1}^{\mathrm{T}}\boldsymbol{\alpha}=1, \tag{22}$$

$$r_k\ge\bar{r}_k, \tag{23}$$

$$0\le\beta_k\le1, \tag{24}$$

$$q_k(r_k)\le Q_k(\alpha_k,\beta_k),\quad k\in\mathcal{K}. \tag{25}$$

In the following sections, we solve the above two formulated problems under the power splitting and time switching modes, respectively. For convenience, Table I summarizes the main notations used in this paper.

III. Power Splitting Receiver

A. Transmission Rate Optimization

1) Problem Analysis and Transformation: According to the power consumption model given in (15), the kth receiver consumes a constant power, v_k, even if it does not receive any information. On the other hand, the problem in (17)–(20) is not meaningful when no information is obtained for any receiver. We have the following proposition.

TABLE I
DEFINITION OF NOTATIONS

Notation	Definition
M	The number of antennas at the BS
K, $\mathcal{K}=\{1,2,\cdots,K\}$	The number and set of receivers
B	System bandwidth
θ_k, $k\in\mathcal{K}$	Channel estimation accuracy of the kth receiver
δ_k, $k\in\mathcal{K}$	Large-scale fading coefficient of the kth receiver
σ_k^2, $k\in\mathcal{K}$	Baseband noise power at the kth receiver
$\boldsymbol{\alpha}=[\alpha_1,\alpha_2,\cdots,\alpha_K]^{\mathrm{T}}$	Power allocation proportions at the BS
$\boldsymbol{\beta}=[\beta_1,\beta_2,\cdots,\beta_K]^{\mathrm{T}}$	Power splitting/time switching factors at the receivers
$\mathbf{r}=[r_1,r_2,\cdots,r_K]^{\mathrm{T}}$	Transmission rate vector of the receivers
$\bar{\mathbf{r}}=[\bar{r}_1,\bar{r}_2,\cdots,\bar{r}_K]^{\mathrm{T}}$	Transmission rate requirement vector of the receivers
p_{T}	Total power consumption of the BS
p	Total transmit power of the PAs at the BS
$E=Mp$	Total power constant at the BS
p_{C}	Circuit power consumption of the BS
ς	Efficiency of PAs at the BS
a	Rate-dependent PCC at the BS
b_0	PCC of complex multiplication operation
b_1	PCC of each RF link
c	Power consumption constant at the BS
Q_k, $k\in\mathcal{K}$	Total harvested power of the kth receiver
ξ_k, $k\in\mathcal{K}$	Energy conversion efficiency at the kth receiver
q_k, $k\in\mathcal{K}$	Total power consumption of the kth receiver
u_k, $k\in\mathcal{K}$	Rate-dependent PCC at the kth receiver
v_k, $k\in\mathcal{K}$	Rate-independent PCC at the kth receiver
η_{EE}	System EE

Proposition 1: In order to guarantee that each receiver has a non-zero transmission rate, the total power constant at the BS should satisfy

$$E>\sum_{k=1}^{K}\frac{v_k}{\xi_k\theta_k\delta_k}. \tag{26}$$

Proof: Based on (7), the harvested power is a monotonically increasing function with respect to the power splitting or time switching factor β_k. Therefore, $\beta_k=1$ $(k\in\mathcal{K})$ results in the maximum harvested power at each receiver, i.e., $Q_k(\alpha_k,1)=\xi_k\alpha_k E\theta_k\delta_k$ for the kth receiver. Then, a non-zero transmission rate can be achieved for the kth receiver only when

$$\xi_k\alpha_k E\theta_k\delta_k>v_k. \tag{27}$$

Further, considering the max-min criterion adopted in (17)–(20) and $\mathbf{1}^{\mathrm{T}}\boldsymbol{\alpha}=1$ leads to (26). ■

Since $q_k(r_k)$ given in (15) is a monotonically increasing function of r_k, equality should hold in (20) in order to maximize the transmission rate of the kth receiver. In order to simplify the problem in (17)–(20) based on $q_k(r_k)=Q_k(\alpha_k,\beta_k)$, we can suppose that the received signal power of the kth receiver in (5) is divided into two parts, i.e., $\alpha_k E\theta_k\delta_k=\tilde{\alpha}_k E\theta_k\delta_k+\bar{\alpha}_k E\theta_k\delta_k$, where

$$\tilde{\alpha}_k=\frac{v_k}{\xi_k\theta_k\delta_k E},\quad \bar{\alpha}_k=\alpha_k-\tilde{\alpha}_k,\ k\in\mathcal{K}. \tag{28}$$

Power $\tilde{\alpha}_k E\theta_k\delta_k$ is used for energy harvesting to satisfy the constant power consumption v_k of the kth receiver, i.e., $\xi_k\tilde{\alpha}_k E\theta_k\delta_k=v_k$. A portion, $\bar{\beta}_k$, of power $\bar{\alpha}_k E\theta_k\delta_k$ is harvested for rate-dependent power consumption $u_k r_k$ at the kth receiver, i.e.,

$$\xi_k\bar{\beta}_k\bar{\alpha}_k E\theta_k\delta_k=u_k r_k; \tag{29}$$

the other portion is transformed into baseband for information decoding and (11) can be rewritten as

$$\rho_k\left(\bar{\alpha}_k,\bar{\beta}_k\right)=\frac{\left(1-\bar{\beta}_k\right)\bar{\alpha}_k E\theta_k\delta_k}{\sigma_k^2}. \tag{30}$$

Therefore, we have

$$\alpha_k=\tilde{\alpha}_k+\bar{\alpha}_k, \tag{31}$$

$$\beta_k=\frac{\tilde{\alpha}_k+\bar{\alpha}_k\bar{\beta}_k}{\tilde{\alpha}_k+\bar{\alpha}_k},\quad k\in\mathcal{K}. \tag{32}$$

Defining $\bar{\boldsymbol{\alpha}}=[\bar{\alpha}_1,\bar{\alpha}_2,\cdots,\bar{\alpha}_K]^{\mathrm{T}}$ and $\tilde{\boldsymbol{\alpha}}=[\tilde{\alpha}_1,\tilde{\alpha}_2,\cdots,\tilde{\alpha}_K]^{\mathrm{T}}$, the problem in (17)–(20) is then transformed into

$$\max_{\bar{\boldsymbol{\alpha}},\bar{\boldsymbol{\beta}}}\min_{k}\ \left\{r_k\left(\bar{\alpha}_k,\bar{\beta}_k\right)\right\} \tag{33}$$

$$\text{s.t. } \mathbf{1}^{\mathrm{T}}\bar{\boldsymbol{\alpha}}=1-\mathbf{1}^{\mathrm{T}}\tilde{\boldsymbol{\alpha}}, \tag{34}$$

$$0\le\bar{\beta}_k\le 1,\quad k\in\mathcal{K}. \tag{35}$$

2) Problem Solution: We have the following results for the power splitting mode.

Theorem 1: For the problem in (33)–(35), the transmission rate r_k of the kth receiver can be expressed as a monotonically increasing function with respect to a single variable $\bar{\alpha}_k$, i.e.,

$$r_k\left(\bar{\alpha}_k\right)=B\log_2\left\{\frac{u_k B}{\xi_k\sigma_k^2\ln 2}\times W_0\left[\frac{\xi_k\sigma_k^2\ln 2}{u_k B}\mathrm{e}^{\frac{\xi_k\sigma_k^2\ln 2}{u_k B}\left(1+\frac{\bar{\alpha}_k E\theta_k\delta_k}{\sigma_k^2}\right)}\right]\right\}. \tag{36}$$

Given the power allocation proportion $\bar{\alpha}_k$, the power splitting factor $\bar{\beta}_k$ can be expressed as

$$\bar{\beta}_k\left(\bar{\alpha}_k\right)=1+\frac{\sigma_k^2}{\bar{\alpha}_k E\theta_k\delta_k}-\frac{u_k B}{\bar{\alpha}_k E\theta_k\delta_k\xi_k\ln 2}\times W_0\left[\frac{\xi_k\sigma_k^2\ln 2}{u_k B}\mathrm{e}^{\frac{\xi_k\sigma_k^2\ln 2}{u_k B}\left(1+\frac{\bar{\alpha}_k E\theta_k\delta_k}{\sigma_k^2}\right)}\right], \tag{37}$$

where $W_0(x):\left[-\mathrm{e}^{-1},\infty\right)\rightarrow[-1,\infty)$ is the first real branch of the Lambert function satisfying $W_0(x)\,\mathrm{e}^{W_0(x)}=x$ [34].

Proof: Substituting (30) into (12) and transforming (29), we have

$$r_k\left(\bar{\alpha}_k,\bar{\beta}_k\right)=B\log_2\left[1+\bar{\alpha}_k\left(1-\bar{\beta}_k\right)\frac{E\theta_k\delta_k}{\sigma_k^2}\right], \tag{38}$$

$$r_k\left(\bar{\alpha}_k,\bar{\beta}_k\right)=\frac{\xi_k\bar{\alpha}_k\bar{\beta}_k E\theta_k\delta_k}{u_k}. \tag{39}$$

Equating the right-hand sides of (38) and (39) and after some manipulations, we have

$$\begin{aligned}&\frac{\xi_k\sigma_k^2\ln 2}{u_kB}\left[1+\left(1-\bar{\beta}_k\right)\frac{\bar{\alpha}_kE\theta_k\delta_k}{\sigma_k^2}\right]\\&\quad\times\exp\left\{\frac{\xi_k\sigma_k^2\ln 2}{u_kB}\left[1+\left(1-\bar{\beta}_k\right)\frac{\bar{\alpha}_kE\theta_k\delta_k}{\sigma_k^2}\right]\right\}\\&=\frac{\xi_k\sigma_k^2\ln 2}{u_kB}\exp\left[\frac{\xi_k\sigma_k^2\ln 2}{u_kB}\left(1+\frac{\bar{\alpha}_kE\theta_k\delta_k}{\sigma_k^2}\right)\right].\end{aligned}\tag{40}$$

Taking advantage of the Lambert function gives rise to

$$\begin{aligned}&1+\left(1-\bar{\beta}_k\right)\frac{\bar{\alpha}_kE\theta_k\delta_k}{\sigma_k^2}\\&=\frac{u_kB}{\xi_k\sigma_k^2\ln 2}W_0\left\{\frac{\xi_k\sigma_k^2\ln 2}{u_kB}\right.\\&\quad\left.\times\exp\left[\frac{\xi_k\sigma_k^2\ln 2}{u_kB}\left(1+\frac{\bar{\alpha}_kE\theta_k\delta_k}{\sigma_k^2}\right)\right]\right\}.\end{aligned}\tag{41}$$

Equation (41) yields (37) and substituting (41) into (38) gives rise to (36).

Since the first real branch of the Lambert function is monotonically increasing, the transmission rate of the kth receiver is a monotonically increasing function of the power allocation proportion $\bar{\alpha}_k$. ■

Theorem 2: In order to maximize the minimum transmission rate of the energy harvesting receivers, the achievable transmission rates of all receivers are the same, given by

$$r=\frac{B}{\ln 2}\left[\Theta-W_0\left(\Omega\mathrm{e}^{\Theta}\right)\right],\tag{42}$$

and the optimal power allocation proportions are given by

$$\alpha_k=\frac{\sigma_k^2}{E\theta_k\delta_k}\left[\mathrm{e}^{\Theta-W_0\left(\Omega\mathrm{e}^{\Theta}\right)}-1\right]+\frac{u_kr+v_k}{\xi_kE\theta_k\delta_k},\quad k\in\mathcal{K},\tag{43}$$

where

$$\Theta=\frac{\ln 2}{B}\left[E+\sum_{k=1}^{K}\frac{1}{\theta_k\delta_k}\left(\sigma_k^2-\frac{v_k}{\xi_k}\right)\right]\bigg/\sum_{k=1}^{K}\frac{u_k}{\xi_k\theta_k\delta_k},\tag{44}$$

$$\Omega=\frac{\ln 2}{B}\sum_{k=1}^{K}\frac{\sigma_k^2}{\theta_k\delta_k}\bigg/\sum_{k=1}^{K}\frac{u_k}{\xi_k\theta_k\delta_k}.\tag{45}$$

Proof: In order to maximize the minimum transmission rate of the energy harvesting receivers, all receivers should have the same transmission rate, i.e.,

$$r_1\left(\bar{\alpha}_1\right)=r_2\left(\bar{\alpha}_2\right)=\cdots=r_K\left(\bar{\alpha}_K\right)\triangleq r.\tag{46}$$

We prove (46) by contradiction. Suppose the optimal solution, $\hat{\boldsymbol{\alpha}}=\left[\hat{\alpha}_1,\hat{\alpha}_2,\cdots,\hat{\alpha}_K\right]^{\mathrm{T}}$ to (33)–(35) is such that

$$r_j\left(\hat{\alpha}_j\right)>r_k\left(\hat{\alpha}_k\right)>r_i\left(\hat{\alpha}_i\right),\quad k\neq i,j.\tag{47}$$

According to *Theorem 1*, both $r_j\left(\cdot\right)$ and $r_i\left(\cdot\right)$ are monotonically increasing functions, there should exist $\Delta\in\left(0,\hat{\alpha}_j\right)$ such that

$$r_j\left(\tilde{\alpha}_j\right)>r_j\left(\tilde{\alpha}_j-\Delta\right)=r_i\left(\tilde{\alpha}_i+\Delta\right)>r_i\left(\tilde{\alpha}_i\right).\tag{48}$$

Then, we can define the new power allocation proportions $\bar{\alpha}_j=\hat{\alpha}_j-\Delta$, $\bar{\alpha}_i=\hat{\alpha}_i+\Delta$, and $\bar{\alpha}_k=\hat{\alpha}_k$ $(k\neq i,j)$ at the BS. With the new power allocation proportions, the minimum transmission rate among all receivers increases, which contradicts with the max-min criterion. Hence, all receivers should have the same transmission rate as per (46).

Expressing $\bar{\beta}_k$ by r_k and $\bar{\alpha}_k$ according to (29) and then substituting $\bar{\beta}_k$ into (38), the transmission rate expression of the kth receiver can be rewritten as

$$r_k\left(\bar{\alpha}_k\right)=B\log_2\left(1+\frac{\bar{\alpha}_kE\xi_k\theta_k\delta_k-u_kr_k}{\xi_k\sigma_k^2}\right),\quad\text{or}\tag{49}$$

$$\bar{\alpha}_k=\frac{u_kr_k+\xi_k\sigma_k^2\left(2^{\frac{r_k}{B}}-1\right)}{\xi_kE\theta_k\delta_k}.\tag{50}$$

Letting $r_k=r$ $(k\in\mathcal{K})$ in (50) and substituting (50) into $\sum_{k=1}^{K}\bar{\alpha}_k=1-\sum_{k=1}^{K}\tilde{\alpha}_k$, we have

$$\left(\Theta-\frac{\ln 2}{B}r\right)\mathrm{e}^{\left(\Theta-\frac{\ln 2}{B}r\right)}=\Omega\mathrm{e}^{\Theta},\tag{51}$$

where Θ and Ω are given by (44) and (45), respectively. Taking advantage of the Lambert function leads to (42).

Substituting (42) into (50) gives rise to

$$\bar{\alpha}_k=\frac{u_kr+\xi_k\sigma_k^2\left\{\exp\left[\Theta-W_0\left(\Omega\mathrm{e}^{\Theta}\right)\right]-1\right\}}{\xi_kE\theta_k\delta_k}.\tag{52}$$

Further substituting (52) into (31) leads to (43). ■

Theorem 2 gives the optimal power allocation proportions at the BS, i.e., α_k in (43). Further substituting (52) into (37) and using (32), we can obtain the optimal power splitting factors β_k at the receivers.

B. Energy Efficiency Optimization

We now consider the EE optimization problem in (21)–(25) for the power splitting mode.

Theorem 3: In order to obtain the optimal EE, η_{EE}^*, of the power splitting mode, the optimal transmit power satisfies

$$p\left(\eta_{\mathrm{EE}}^*\right)=\sum_{k=1}^{K}\frac{\sigma_k^2\xi_k\left[2^{\frac{r_k\left(\eta_{\mathrm{EE}}^*\right)}{B}}-1\right]+u_kr_k\left(\eta_{\mathrm{EE}}^*\right)+v_k}{M\xi_k\theta_k\delta_k}.\tag{53}$$

Moreover, the optimal power allocation proportions at the BS and the power splitting factors at the receivers are respectively given by

$$\alpha_k\left(\eta_{\mathrm{EE}}^*\right)=\frac{\sigma_k^2\xi_k\left[2^{\frac{r_k\left(\eta_{\mathrm{EE}}^*\right)}{B}}-1\right]+u_kr_k\left(\eta_{\mathrm{EE}}^*\right)+v_k}{M\xi_k\theta_k\delta_kp\left(\eta_{\mathrm{EE}}^*\right)},\tag{54}$$

$$\beta_k\left(\eta_{\mathrm{EE}}^*\right)=\frac{u_kr_k\left(\eta_{\mathrm{EE}}^*\right)+v_k}{M\xi_k\theta_k\delta_k\alpha_k\left(\eta_{\mathrm{EE}}^*\right)p\left(\eta_{\mathrm{EE}}^*\right)},\tag{55}$$

where $r_k\left(\eta_{\mathrm{EE}}^*\right)=\max\left\{\tilde{r}_k\left(\eta_{\mathrm{EE}}^*\right),\bar{r}_k\right\}$ with

$$\tilde{r}_k\left(\eta_{\mathrm{EE}}^*\right)=B\log_2\left[\frac{\varsigma M\xi_k\theta_k\delta_k\left(1/\eta_{\mathrm{EE}}^*-a\right)-u_k}{\xi_k\sigma_k^2\ln 2/B}\right].\tag{56}$$

Proof: The problem in (21)–(25) is non-convex with respect to transmit power p, power allocation proportions $\boldsymbol{\alpha}$ and power splitting factors $\boldsymbol{\beta}$. Therefore, we first transform the objective $\eta_{\mathrm{EE}}\left(p,\boldsymbol{\alpha},\boldsymbol{\beta}\right)$ into a quasi-convex function with respect to the transmission rate vector $\mathbf{r}=\left[r_1,r_2,\cdots,r_K\right]^{\mathrm{T}}$. Then, (21)–(25) can be rewritten into an equivalent convex problem.

According to (7) and (12), the allocated power at the BS for energy harvesting and information decoding of the kth receiver can be respectively written as

$$p_{\mathrm{E}k}(r_k) = \frac{u_k r_k + v_k}{M\xi_k\theta_k\delta_k}, \tag{57}$$

$$p_{\mathrm{I}k}(r_k) = \frac{\sigma_k^2}{M\theta_k\delta_k}\left(2^{\frac{r_k}{B}} - 1\right). \tag{58}$$

Then, the total transmit power at the BS is

$$p(\mathbf{r}) = \sum_{k=1}^{K}[p_{\mathrm{I}k}(r_k) + p_{\mathrm{E}k}(r_k)], \tag{59}$$

and the power allocation proportion and power splitting factor for the kth receiver are respectively given by

$$\alpha_k(\mathbf{r}) = \frac{p_{\mathrm{I}k}(r_k) + p_{\mathrm{E}k}(r_k)}{p(\mathbf{r})}, \tag{60}$$

$$\beta_k(\mathbf{r}) = \frac{u_k r_k + v_k}{M\xi_k\theta_k\delta_k\alpha_k(\mathbf{r})\, p(\mathbf{r})}. \tag{61}$$

Further, the system EE in (16) can be rewritten into a function of the transmission rate vector, i.e.,

$$\eta_{\mathrm{EE}}(\mathbf{r}) = \frac{\mathbf{1}^{\mathrm{T}}\mathbf{r}}{p_{\mathrm{T}}(\mathbf{r})} = \left[a + \frac{f(\mathbf{r})}{\mathbf{1}^{\mathrm{T}}\mathbf{r}}\right]^{-1}, \tag{62}$$

where

$$f(\mathbf{r}) = \frac{1}{\varsigma M}\sum_{k=1}^{K}\frac{1}{\theta_k\delta_k}\left[\sigma_k^2\left(2^{\frac{r_k}{B}} - 1\right) + \frac{u_k r_k + v_k}{\xi_k}\right] + M(b_0 + b_1 K) + c. \tag{63}$$

Therefore, (21)–(25) can be transformed into

$$\min_{\mathbf{r}} \quad \left\{\eta_{\mathrm{EE}}^{-1}(\mathbf{r})\right\} \tag{64}$$

$$\text{s.t. } r_k \geq \bar{r}_k, \quad k \in \mathcal{K}. \tag{65}$$

The Hessian matrix of $f(\mathbf{r})$ with respect to $\mathbf{r}$ is given by

$$\nabla^2 f(\boldsymbol{r}) = \frac{1}{\varsigma M}\left(\frac{\ln 2}{B}\right)^2 \mathrm{diag}\left\{\frac{\sigma_1^2}{\theta_1\delta_1}\mathrm{e}^{\frac{r_1\ln 2}{B}}, \frac{\sigma_2^2}{\theta_2\delta_2}\mathrm{e}^{\frac{r_2\ln 2}{B}}, \cdots, \times\frac{\sigma_K^2}{\theta_K\delta_K}\mathrm{e}^{\frac{r_K\ln 2}{B}}\right\} \succeq 0, \tag{66}$$

therefore $f(\mathbf{r})$ is convex with respect to $\mathbf{r}$. On the other hand, $\mathbf{1}^{\mathrm{T}}\mathbf{r}$ is an affine function with respect to $\mathbf{r}$, therefore the set $\left\{\mathbf{r}|\eta_{\mathrm{EE}}^{-1} - a = f(\mathbf{r})/\left(\mathbf{1}^{\mathrm{T}}\mathbf{r}\right) \leq e\right\}$ is convex and $\eta_{\mathrm{EE}}^{-1}(\mathbf{r})$ is a quasi-convex function with respect to $\mathbf{r}$. Based on [35]–[37], if the fractional objective given in (64) is quasi-convex with the convex numerator and affine denominator, the optimization problem in (64)–(65) is equivalent to

$$\min_{\mathbf{r}} \quad J(\mathbf{r}, \eta_{\mathrm{EE}}) \triangleq f(\mathbf{r}) - \left(\eta_{\mathrm{EE}}^{-1} - a\right)\mathbf{1}^{\mathrm{T}}\mathbf{r} \tag{67}$$

$$\text{s.t. } r_k \geq \bar{r}_k, \quad k \in \mathcal{K}, \tag{68}$$

and the optimal system EE η_{EE}^* in (64)–(65) satisfies

$$J(\mathbf{r}, \eta_{\mathrm{EE}}) \begin{cases} >0, & \eta_{\mathrm{EE}} > \eta_{\mathrm{EE}}^*, \\ =0, & \eta_{\mathrm{EE}} = \eta_{\mathrm{EE}}^*, \\ <0, & \eta_{\mathrm{EE}} < \eta_{\mathrm{EE}}^*. \end{cases} \tag{69}$$

Given η_{EE}, the Lagrange function of (67)–(68) is given by

$$\mathcal{L}(\mathbf{r}; \boldsymbol{\lambda}) = f(\mathbf{r}) - \left(\eta_{\mathrm{EE}}^{-1} - a\right)\mathbf{1}^{\mathrm{T}}\mathbf{r} - \boldsymbol{\lambda}^{\mathrm{T}}(\mathbf{r} - \bar{\mathbf{r}}), \tag{70}$$

where $\boldsymbol{\lambda} = [\lambda_1, \lambda_2, \cdots, \lambda_K]^{\mathrm{T}}$ is the Lagrange multiplier vector. Applying the Karush-Kuhn-Tucker (KKT) conditions [35], we can obtain

$$r_k = B\log_2\left[\frac{\varsigma M\xi_k\theta_k\delta_k\left(\eta_{\mathrm{EE}}^{-1} - a + \lambda_k\right) - u_k}{\xi_k\sigma_k^2\ln 2/B}\right], \tag{71}$$

$$\lambda_k(r_k - \bar{r}_k) = 0, \quad k \in \mathcal{K}, \tag{72}$$

which lead to

$$r_k(\eta_{\mathrm{EE}}) = \max\left\{B\log_2\left[\frac{\varsigma M\xi_k\theta_k\delta_k\left(\eta_{\mathrm{EE}}^{-1} - a\right) - u_k}{\xi_k\sigma_k^2\ln 2/B}\right], \bar{r}_k\right\}. \tag{73}$$

Substituting (73) into (59), (60) and (61) results in (53) and (54) and (55), respectively. On the other hand, the optimal EE η_{EE}^* can be obtained by bi-section search according to (69). ■

Based on *Theorem 3* and (69), a bi-section search algorithm for the optimal system EE, η_{EE}^*, is given in Algorithm 1, where the initial values of $\eta_{\mathrm{EE}}^{\mathrm{L}}$ and $\eta_{\mathrm{EE}}^{\mathrm{U}}$ should constitute a range such that $\eta_{\mathrm{EE}}^* \in \left(\eta_{\mathrm{EE}}^{\mathrm{L}}, \eta_{\mathrm{EE}}^{\mathrm{U}}\right)$. According to (62), $\eta_{\mathrm{EE}}^* \leq 1/a$ and therefore we can set $\eta_{\mathrm{EE}}^{\mathrm{U}} = 1/a$. On the other hand, $\eta_{\mathrm{EE}}(\mathbf{r})$ is a quasi-concave function, any $\mathbf{r} \succeq \bar{\mathbf{r}}$ can satisfy $\eta_{\mathrm{EE}}^{\mathrm{L}} = \eta_{\mathrm{EE}}(\mathbf{r}) \leq \eta_{\mathrm{EE}}^*$ and we set $\mathbf{r} = \bar{\mathbf{r}}$ in Algorithm 1.

Algorithm 1 Bi-Section Search Algorithm for Solving the EE Optimization Problem in (21)–(25) Under Power Splitting Mode

Step 1: Initialize $\eta_{\mathrm{EE}}^{\mathrm{L}} = \eta_{\mathrm{EE}}(\bar{\mathbf{r}}) \leq \eta_{\mathrm{EE}}^*$, $\eta_{\mathrm{EE}}^{\mathrm{U}} = 1/a \geq \eta_{\mathrm{EE}}^*$, and error tolerance $\epsilon > 0$.

Step 2: Let $\eta_{\mathrm{EE}} = \left(\eta_{\mathrm{EE}}^{\mathrm{L}} + \eta_{\mathrm{EE}}^{\mathrm{U}}\right)/2$ and compute $r_k(\eta_{\mathrm{EE}})$ in (73) and $J(\mathbf{r}, \eta_{\mathrm{EE}})$ in (67).
If $J(\mathbf{r}, \eta_{\mathrm{EE}}) > 0$, then $\eta_{\mathrm{EE}}^{\mathrm{U}} = \eta_{\mathrm{EE}}$;
Else $\eta_{\mathrm{EE}}^{\mathrm{L}} = \eta_{\mathrm{EE}}$.

Step 3: If $\eta_{\mathrm{EE}}^{\mathrm{U}} - \eta_{\mathrm{EE}}^{\mathrm{L}} < \epsilon$, let $\eta_{\mathrm{EE}}^* = \left(\eta_{\mathrm{EE}}^{\mathrm{L}} + \eta_{\mathrm{EE}}^{\mathrm{U}}\right)/2$;
Else go to Step 2.

Step 4: Calculate p, α_k and β_k $(k \in \mathcal{K})$ according to (53), (54) and (55), respectively.

IV. TIME SWITCHING RECEIVER

A. Transmission Rate Optimization

1) Problem Analysis: Whether the power splitting or time switching mode is employed at the receivers, the constant power consumption of the receivers always holds. Therefore, *Proposition 1* should also be satisfied under the time switching mode. We have the following results when the energy harvesting receivers adopt the time switching mode.

Theorem 4: For the energy harvesting receivers, the time switching factor β_k is a monotonically decreasing function with respect to the power allocation proportion α_k, i.e.,

$$\beta_k(\alpha_k) = \frac{u_k B\log_2\left(1 + \frac{\alpha_k E\theta_k\delta_k}{\sigma_k^2}\right) + v_k}{\xi_k\alpha_k E\theta_k\delta_k - u_k B\log_2\left(1 + \frac{\alpha_k E\theta_k\delta_k}{\sigma_k^2}\right)}, \tag{74}$$

where $\alpha_k \in (\underline{\alpha}_k, 1)$ and

$$\underline{\alpha}_k = \frac{1}{E\theta_k\delta_k}\max\left\{\frac{v_k}{\xi_k}, -\sigma_k^2 - \frac{2u_kB}{\xi_k\ln 2}\right.$$
$$\left.\times W_{-1}\left[-\frac{\xi_k\sigma_k^2\ln 2}{2u_kB}\mathrm{e}^{-\frac{\xi_k\ln 2}{2u_kB}\left(\frac{v_k}{\xi_k}+\sigma_k^2\right)}\right]\right\}, \quad (75)$$

and $W_{-1}(x) : [-\mathrm{e}^{-1}, 0) \rightarrow [-1, -\infty)$ is the second real branch of the Lambert function satisfying $W_{-1}(x)\mathrm{e}^{W_{-1}(x)} = x$ [34]. Moreover, the transmission rate of the kth receiver is a monotonically increasing function with respect to the power allocation proportion α_k only, i.e.,

$$r_k(\alpha_k) = [1 - \beta_k(\alpha_k)]B\log_2\left(1 + \frac{\alpha_kE\theta_k\delta_k}{\sigma_k^2}\right). \quad (76)$$

Proof: Substituting (7) and (12) into $Q_k(r_k) = u_kr_k + v_k$, we can obtain $\beta_k(\alpha_k)$ given in (74). Taking into account $\beta_k(\alpha_k) \in [0, 1]$, we have

$$u_kB\log_2\left(1 + \frac{\alpha_kE\theta_k\delta_k}{\sigma_k^2}\right) + v_k$$
$$< \xi_k\alpha_kE\theta_k\delta_k - u_kB\log_2\left(1+\frac{\alpha_kE\theta_k\delta_k}{\sigma_k^2}\right), \quad (77)$$

$$\xi_k\alpha_kE\theta_k\delta_k > u_kB\log_2\left(1 + \frac{\alpha_kE\theta_k\delta_k}{\sigma_k^2}\right). \quad (78)$$

It is easy to see that (78) holds if (77) is satisfied. Under the condition $\xi_k\alpha_kE\theta_k\delta_k > v_k$, (77) can be transformed into

$$-\frac{\xi_k\ln 2}{2u_kB}\left(\alpha_kE\theta_k\delta_k + \sigma_k^2\right)\exp\left[-\frac{\xi_k\ln 2}{2u_kB}\left(\alpha_kE\theta_k\delta_k + \sigma_k^2\right)\right]$$
$$> -\frac{\xi_k\ln 2}{2u_kB}\sigma_k^2\exp\left[-\frac{\xi_k\ln 2}{2u_kB}\left(\frac{v_k}{\xi_k} + \sigma_k^2\right)\right]. \quad (79)$$

Then, according to the definition of the Lambert function [34], we have

$$\alpha_k > -\frac{2u_kBW_{-1}\left\{-\frac{\xi_k\ln 2}{2u_kB}\sigma_k^2\exp\left[-\frac{\xi_k\ln 2}{2u_kB}\left(\frac{v_k}{\xi_k}+\sigma_k^2\right)\right]\right\}}{E\theta_k\delta_k\xi_k\ln 2}$$
$$-\frac{\sigma_k^2}{E\theta_k\delta_k}. \quad (80)$$

Taking into account $\xi_k\alpha_kE\theta_k\delta_k > v_k$ yields $\alpha_k \in (\underline{\alpha}_k, 1)$, where $\underline{\alpha}_k$ is given by (75).

Ignoring upper and lower limits of α_k, (74) can be further rewritten as

$$\beta_k(\alpha_k) = \frac{\frac{v_k}{u_kB\log_2\left(1+\frac{\alpha_kE\theta_k\delta_k}{\sigma_k^2}\right)} + 1}{\frac{\xi_k\alpha_kE\theta_k\delta_k}{u_kB\log_2\left(1+\frac{\alpha_kE\theta_k\delta_k}{\sigma_k^2}\right)} - 1}. \quad (81)$$

Denoting

$$f_k(\alpha_k) = \frac{\xi_k\alpha_kE\theta_k\delta_k}{u_kB\log_2\left(1 + \frac{\alpha_kE\theta_k\delta_k}{\sigma_k^2}\right)} - 1. \quad (82)$$

Then its derivative is given by

$$\frac{\mathrm{d}f_k(\alpha_k)}{\mathrm{d}\alpha_k} = \frac{\xi E\theta_k\delta_k}{u_kB\ln 2}\left[\log_2\left(1 + \frac{\alpha_kE\theta_k\delta_k}{\sigma_k^2}\right)\right]^{-2}$$
$$\times\left[\ln\left(1 + \frac{\alpha_kE\theta_k\delta_k}{\sigma_k^2}\right) - \frac{\frac{\alpha_kE\theta_k\delta_k}{\sigma_k^2}}{1 + \frac{\alpha_kE\theta_k\delta_k}{\sigma_k^2}}\right]. \quad (83)$$

Noting $\rho_k = \alpha_kE\theta_k\delta_k/\sigma_k^2 > 0$, we have

$$\frac{\mathrm{d}\ln(1+\rho_k)}{\mathrm{d}\rho_k} = \frac{1}{1+\rho_k} > \frac{\mathrm{d}}{\mathrm{d}\rho_k}\left(\frac{\rho_k}{1+\rho_k}\right) = \frac{1}{(1+\rho_k)^2}, \quad (84)$$

and

$$\ln(1+\rho_k)|_{\rho_k=0} = 0 = \left.\frac{\rho_k}{1+\rho_k}\right|_{\rho_k=0}, \quad (85)$$

therefore $\mathrm{d}f_k(\alpha_k)/\mathrm{d}\alpha_k > 0$ and the denominator of (81) is an increasing function with respect to α_k. On the other hand, the numerator of (81) is a decreasing function with respect to α_k. Therefore, $\beta_k(\alpha_k)$ is a decreasing function with respect to the power allocation proportion α_k.

Substituting (74) into (12), we obtain (76). Since both $1 - \beta_k(\alpha_k)$ and $\log_2(1 + \alpha_kE\theta_k\delta_k/\sigma_k^2)$ are increasing functions of α_k, then $r_k(\alpha_k)$ is an increasing function with respect to α_k. ■

Following the same line as in the proof of *Theorem 2*, we have

$$r_1(\alpha_1) = r_2(\alpha_2) = \cdots = r_K(\alpha_K) \triangleq r. \quad (86)$$

However, we can not obtain the closed-form expression of α_k by solving the transcendental equation, i.e., (76). Therefore, when the time switching mode is adopted by the energy harvesting receivers, we need to develop an algorithm to solve the problem in (17)–(20).

2) Algorithm Description: Based on *Theorem 4* and (86), an iterative power allocation algorithm is proposed for solving (17)–(20), which is described as follows. Let $\mathbf{r}^{t-1} = \left[r_1^{t-1}, r_2^{t-1}, \cdots, r_K^{t-1}\right]^{\mathrm{T}}$ contain the transmission rates of all receivers in the $(t-1)\mathrm{th}$ iteration. In the $t\mathrm{th}$ iteration, the BS first calculates $k_{\mathrm{m}}^t = \arg\min\left\{\mathbf{r}^{t-1}\right\}$ and $k_{\mathrm{M}}^t = \arg\max\left\{\mathbf{r}^{t-1}\right\}$; then increases the power allocation proportion of the $k_{\mathrm{m}}^t\mathrm{th}$ receiver by Δ^{t-1} and simultaneously reduces that of the $k_{\mathrm{M}}^t\mathrm{th}$ receiver by the same amount in order to satisfy $\mathbf{1}^{\mathrm{T}}\boldsymbol{\alpha} = 1$. Thus, the minimum transmission rate increases, while simultaneously the maximum transmission rate decreases in each iteration until all receivers have the same transmission rate, i.e., $\lim_{t\to\infty}(r_{k_{\mathrm{M}}^t}^t - r_{k_{\mathrm{m}}^t}^t) \rightarrow 0$.

Initialized with equal power allocation at the BS, the iterative power allocation algorithm for time switching mode is summarized in Algorithm 2, where the objective of the "If" statement in Step 5 is to avoid the ping-pong phenomenon between the $k_{\mathrm{m}}^t\mathrm{th}$ and $k_{\mathrm{M}}^t\mathrm{th}$ receivers.

Note that $|r_k(\alpha_k) - r| \leq \frac{\epsilon}{2}$ is a sufficient condition for Algorithm 2 to stop based on the termination condition $\max\{\mathbf{r}^t\} - \min\{\mathbf{r}^t\} \leq \epsilon$. Then, we have $\alpha_k^{\mathrm{L}}(\epsilon) \leq \alpha_k \leq \alpha_k^{\mathrm{H}}(\epsilon)$ with $\alpha_k^{\mathrm{L}}(\epsilon) = r_k^{-1}\left(r - \frac{\epsilon}{2}\right)$ and $\alpha_k^{\mathrm{H}}(\epsilon) = r_k^{-1}\left(r + \frac{\epsilon}{2}\right)$. Denoting T_k as the number of iterations for the kth receiver, then we have $\frac{\Delta^0}{2^{T_k+1}} \leq \alpha_k^{\mathrm{H}}(\epsilon) - \alpha_k^{\mathrm{L}}(\epsilon) \leq \frac{\Delta^0}{2^{T_k}}$, i.e., $T_k \sim \mathcal{O}\left(\log_2\left[r_k^{-1}\left(r+\frac{\epsilon}{2}\right) - r_k^{-1}\left(r-\frac{\epsilon}{2}\right)\right]^{-1}\right)$.

B. Energy Efficiency Optimization

Similar to the EE optimization under the power splitting mode discussed in Section III-B, we first transform the problem in (21)–(25) under the time switching mode into a convex

Algorithm 2 Iterative Algorithm for Solving the Max-Min Transmission Rate Problem in (17)–(20) Under Time Switching Mode

Initialization:

- Error tolerance $\epsilon > 0$, adjustable power proportion $\Delta^0 \in (0,1)$, power allocation proportions $\alpha_k^0 = \tilde{\alpha}_k + (1 - \sum_{k=1}^K \tilde{\alpha}_k)/K$ $(k \in \mathcal{K})$ and $t = 0$.
- Calculate the transmission rate vector $\mathbf{r}^0 = \left[r_1^0, r_2^0, \cdots, r_K^0\right]^{\mathrm{T}}$ using (76).

Do {**Step 1:** $t \leftarrow t+1$.

Step 2: Calculate $k_{\mathrm{m}}^t = \arg\min\left\{\mathbf{r}^{t-1}\right\}$ and $k_{\mathrm{M}}^t = \arg\max\left\{\mathbf{r}^{t-1}\right\}$.

Step 3: Update $\alpha_{k_{\mathrm{m}}^t}^t = \alpha_{k_{\mathrm{m}}^t}^{t-1} + \Delta^{t-1}$ and $\alpha_{k_{\mathrm{M}}^t}^t = \alpha_{k_{\mathrm{M}}^t}^{t-1} - \Delta^{t-1}$.

Step 4: Calculate $r_{k_{\mathrm{m}}^t}^t$ and $r_{k_{\mathrm{M}}^t}^t$ according to (76).

Step 5: **If** $r_{k_{\mathrm{m}}^t}^t \le r_{k_{\mathrm{m}}^t}^{t-1}$ or $r_{k_{\mathrm{M}}^t}^t \ge r_{k_{\mathrm{M}}^t}^{t-1}$ or $\bar{\alpha}_{k_{\mathrm{M}}^t}^t \le 0$

{Update $\Delta^t = \Delta^{t-1}/2$, $\mathbf{r}^t = \mathbf{r}^{t-1}$, $\alpha_{k_{\mathrm{m}}^t}^t = \alpha_{k_{\mathrm{m}}^t}^{t-1}$ and $\alpha_{k_{\mathrm{M}}^t}^t = \alpha_{k_{\mathrm{M}}^t}^{t-1}$.}

Else {Update $\Delta^t = \Delta^{t-1}$ and $\mathbf{r}^t$ with $r_{k_{\mathrm{m}}^t}^t$, $r_{k_{\mathrm{M}}^t}^t$ and $r_k^t = r_k^{t-1}$ $(k \ne k_{\mathrm{m}}^t, k_{\mathrm{M}}^t)$.} }

While $\max\left\{\mathbf{r}^t\right\} - \min\left\{\mathbf{r}^t\right\} \ge \epsilon$

With the obtained $\boldsymbol{\alpha}^t = \left[\alpha_1^t, \alpha_2^t, \cdots, \alpha_K^t\right]^{\mathrm{T}}$, we can calculate $\boldsymbol{\beta}^t = \left[\beta_1^t, \beta_2^t, \cdots, \beta_K^t\right]^{\mathrm{T}}$ using (74).

problem with respect to the transmission rates and power splitting factors, and then propose an algorithm to optimize the system EE.

1) Problem Transformation: According to the transmission rate expression of time switching mode in (12) and combining the power consumption model in (15) with the energy harvesting expression in (7), we obtain the transmit power expressions for information transmission and energy transfer during a coherence time interval T, given respectively by

$$\alpha_k p = p_{\mathrm{I}k}(r_k, \beta_k) \triangleq \frac{\sigma_k^2}{M\theta_k\delta_k}\left[2^{\frac{r_k}{B(1-\beta_k)}} - 1\right], \quad \beta_k T \le t \le T, \tag{87}$$

$$\alpha_k p = p_{\mathrm{E}k}(r_k, \beta_k) \triangleq \frac{u_k r_k + v_k}{M\beta_k\xi_k\theta_k\delta_k}, \quad 0 \le t \le \beta_k T,\ k \in \mathcal{K}. \tag{88}$$

Equating the right-hand sides of (87) and (88), we have

$$g_k(r_k, \beta_k) \triangleq \frac{\beta_k\sigma_k^2}{\theta_k\delta_k}\left[2^{\frac{r_k}{B(1-\beta_k)}} - 1\right] - \frac{u_k r_k + v_k}{\xi_k\theta_k\delta_k} = 0. \tag{89}$$

Further, the total transmit power of the BS is given by

$$p(\mathbf{r}, \boldsymbol{\beta}) = \sum_{k=1}^K p_{\mathrm{I}k}(r_k, \beta_k) = \sum_{k=1}^K p_{\mathrm{E}k}(r_k, \beta_k), \tag{90}$$

and the power allocation proportion can be expressed as

$$\alpha_k(\mathbf{r}, \boldsymbol{\beta}) = \frac{p_{\mathrm{I}k}(r_k, \beta_k)}{p(\mathbf{r}, \boldsymbol{\beta})} = \frac{p_{\mathrm{E}k}(r_k, \beta_k)}{p(\mathbf{r}, \boldsymbol{\beta})}. \tag{91}$$

Substituting (90) into the total power consumption model in (13) and based on the definition of EE in (16), we have

$$\eta_{\mathrm{EE}}(\mathbf{r}, \boldsymbol{\beta}) = \frac{\mathbf{1}^{\mathrm{T}}\mathbf{r}}{p_{\mathrm{T}}(\mathbf{r}, \boldsymbol{\beta})} = \left[a + \frac{f(\mathbf{r}, \boldsymbol{\beta})}{\mathbf{1}^{\mathrm{T}}\mathbf{r}}\right]^{-1}, \tag{92}$$

where

$$f(\mathbf{r}, \boldsymbol{\beta}) = \frac{1}{\varsigma M}\sum_{k=1}^K \frac{\sigma_k^2}{\theta_k\delta_k}\left[2^{\frac{r_k}{B(1-\beta_k)}} - 1\right] + M(b_0 + b_1 K) + c. \tag{93}$$

Then, the EE optimization problem in (21)–(25) can be transformed into

$$\min_{\mathbf{r}, \boldsymbol{\beta}} \ \eta_{\mathrm{EE}}^{-1}(\mathbf{r}, \boldsymbol{\beta}) \tag{94}$$

$$\text{s.t. } r_k \ge \bar{r}_k, \tag{95}$$

$$g_k(r_k, \beta_k) = 0, \quad k \in \mathcal{K}. \tag{96}$$

Compared with the EE optimization problem in (64)–(65) under the power splitting mode, (94)–(96) is an optimization problem with respect to $\mathbf{r}$ and $\boldsymbol{\beta}$ under the time switching mode because we can not obtain the closed-form expression of β_k with respect to r_k by solving the transcendental equation, i.e., (89) or (96).

Following the similar derivation as in the proof of *Theorem 3*, the problem in (94)–(96) can be rewritten as

$$\begin{aligned}&\min_{\mathbf{r}, \boldsymbol{\beta}} \ J(\mathbf{r}, \boldsymbol{\beta}, \eta_{\mathrm{EE}}) \triangleq f(\mathbf{r}, \boldsymbol{\beta}) - \left(\eta_{\mathrm{EE}}^{-1} - a\right)\mathbf{1}^{\mathrm{T}}\mathbf{r}\\ &\text{s.t. } (95) \text{ and } (96),\end{aligned} \tag{97}$$

and the system EE satisfies

$$J(\mathbf{r}, \boldsymbol{\beta}, \eta_{\mathrm{EE}}) \begin{cases} > 0, & \eta_{\mathrm{EE}} > \eta_{\mathrm{EE}}^*, \\ = 0, & \eta_{\mathrm{EE}} = \eta_{\mathrm{EE}}^*, \\ < 0, & \eta_{\mathrm{EE}} < \eta_{\mathrm{EE}}^*. \end{cases} \tag{98}$$

According to (98), we can use the bi-section search to find the optimal EE if we can find the optimal transmission rates and time switching factors for fixed EE.

2) Optimal Energy Efficiency: In order to obtain the optimal transmission rates and time switching factors, the Lagrange dual method is employed to solve the problem in (97). The Lagrange function of (97) is given by

$$\begin{aligned}\mathcal{L}(\mathbf{r}, \boldsymbol{\beta}; \boldsymbol{\lambda}, \boldsymbol{\mu}) = {} & f(\mathbf{r}, \boldsymbol{\beta}) - \left(\eta_{\mathrm{EE}}^{-1} - a\right)\mathbf{1}^{\mathrm{T}}\mathbf{r} - \boldsymbol{\lambda}^{\mathrm{T}}(\mathbf{r} - \bar{\mathbf{r}}) \\ & + \sum_{k=1}^K \mu_k g_k(r_k, \beta_k),\end{aligned} \tag{99}$$

where $\boldsymbol{\lambda} = [\lambda_1, \lambda_2, \cdots, \lambda_K]^{\mathrm{T}} \succeq \mathbf{0}$ and $\boldsymbol{\mu} = [\mu_1, \mu_2, \cdots, \mu_K]^{\mathrm{T}}$ are the Lagrange multiplier vectors.

Theorem 5: Given η_{EE}, the optimal transmission rate $\mathbf{r}$ and power splitting factor $\boldsymbol{\beta}$ in (97) can be obtained by iterating between $\{\mathbf{r}, \boldsymbol{\beta}\}$ and $\{\boldsymbol{\lambda}, \boldsymbol{\mu}\}$ as follows. Given $\boldsymbol{\lambda}$ and $\boldsymbol{\mu}$, the transmission rate and power splitting factor are given respectively by

$$r_k(\lambda_k,\mu_k) = \frac{B}{\ln 2}\left(1+\frac{1}{\mu_k\varsigma M}\right) \times \frac{\Phi_k(\lambda_k,\mu_k)\Psi_k(\lambda_k,\mu_k)\exp\{\Phi_k(\lambda_k,\mu_k)\}}{1+\Psi_k(\lambda_k,\mu_k)\exp\{\Phi_k(\lambda_k,\mu_k)\}}, \tag{100}$$

$$\beta_k(\lambda_k,\mu_k) = \frac{1}{\mu_k\varsigma M}\frac{\mu_k\varsigma M-\Psi_k(\lambda_k,\mu_k)\exp\{\Phi_k(\lambda_k,\mu_k)\}}{1+\Psi_k(\lambda_k,\mu_k)\exp\{\Phi_k(\lambda_k,\mu_k)\}}, \tag{101}$$

where

$$\Psi_k(\lambda_k,\mu_k) = \frac{\mu_k\xi_k\sigma_k^2\ln 2}{B\left[\mu_k u_k+\xi_k\theta_k\delta_k\left(\eta_{\mathrm{EE}}^{-1}-a+\lambda_k\right)\right]}, \tag{102}$$

$$\Phi_k(\lambda_k,\mu_k) = \Psi_k(\lambda_k,\mu_k) - W_{-1}\left[\Psi_k(\lambda_k,\mu_k)\,\mathrm{e}^{\Psi_k(\lambda_k,\mu_k)}\right]. \tag{103}$$

Given $\mathbf{r}$ and $\boldsymbol{\beta}$, the Lagrange multipliers are updated as

$$\lambda_k^t = \lambda_k^{t-1} + \kappa_k^1(r_k-\bar{r}_k), \tag{104}$$

$$\mu_k^t = \mu_k^{t-1} - \kappa_k^2 g_k(r_k,\beta_k), \tag{105}$$

where κ_k^1 and κ_k^2 $(k\in\mathcal{K})$ are the step sizes.

Proof: The dual function and dual problem of (99) are given respectively by

$$\phi(\boldsymbol{\lambda},\boldsymbol{\mu}) = \min_{\boldsymbol{r},\boldsymbol{\beta}} \ \{\mathcal{L}(\boldsymbol{r},\boldsymbol{\beta};\boldsymbol{\lambda},\boldsymbol{\mu})\}, \tag{106}$$

and

$$\max_{\boldsymbol{\lambda},\boldsymbol{\mu}} \ \{\phi(\boldsymbol{\lambda},\boldsymbol{\mu})\} \quad \text{s.t. } \boldsymbol{\lambda}\succeq 0. \tag{107}$$

According to the KKT conditions [35], we have

$$\frac{\partial\mathcal{L}}{\partial r_k} = \frac{\sigma_k^2}{\theta_k\delta_k}\frac{\ln 2}{B(1-\beta_k)}\left(\frac{1}{\varsigma M}+\mu_k\beta_k\right)\mathrm{e}^{\frac{r_k\ln 2}{B(1-\beta_k)}} - \frac{\mu_k u_k}{\xi_k\theta_k\delta_k} - \left(\eta_{\mathrm{EE}}^{-1}-a+\lambda_k\right) = 0, \tag{108}$$

$$\frac{\partial\mathcal{L}}{\partial \beta_k} = \frac{\sigma_k^2}{\theta_k\delta_k}\frac{r_k\ln 2}{B(1-\beta_k)^2}\left(\frac{1}{\varsigma M}+\mu_k\beta_k\right)\mathrm{e}^{\frac{r_k\ln 2}{B(1-\beta_k)}} + \frac{\mu_k\sigma_k^2}{\theta_k\delta_k}\left[\mathrm{e}^{\frac{r_k\ln 2}{B(1-\beta_k)}}-1\right] = 0, \quad k\in\mathcal{K}. \tag{109}$$

Combining (108) and (109) yields

$$\left[\Psi_k(\lambda_k,\mu_k) - \frac{r_k\ln 2}{B(1-\beta_k)}\right]\mathrm{e}^{\Psi_k(\lambda_k,\mu_k)-\frac{r_k\ln 2}{B(1-\beta_k)}} = \Psi_k(\lambda_k,\mu_k)\,\mathrm{e}^{\Psi_k(\lambda_k,\mu_k)}. \tag{110}$$

According to the definition of the Lambert function, we obtain

$$\frac{r_k\ln 2}{B(1-\beta_k)} = \Psi_k(\lambda_k,\mu_k) - W_{-1}\left[\Psi_k(\lambda_k,\mu_k)\,\mathrm{e}^{\Psi_k(\lambda_k,\mu_k)}\right], \tag{111}$$

where $\Psi_k(\lambda_k,\mu_k)<0$, i.e.,

$$\mu_k \in \left(-\frac{\xi_k\theta_k\delta_k\left(\eta_{\mathrm{EE}}^{-1}-a+\lambda_k\right)}{u_k}, 0\right). \tag{112}$$

Substituting (111) into (108) gives rise to (101), and further substituting (101) into (111) results in (100).

The Lagrange multipliers can be updated by the subgradient method [38]. The update rates are given by

$$\frac{\partial\mathcal{L}}{\partial\lambda_k} = -(r_k-\bar{r}_k), \tag{113}$$

$$\frac{\partial\mathcal{L}}{\partial\mu_k} = g_k(r_k,\beta_k), \quad k\in\mathcal{K}, \tag{114}$$

which lead to (104) and (105). ■

Algorithm 3 Iterative Algorithm for Solving the EE Optimization Problem in (21)–(25) Under Time Switching Mode

Step 1: Initialize $\eta_{\mathrm{EE}}^{\mathrm{L}} = \eta_{\mathrm{EE}}(\bar{\mathbf{r}},\mathbf{1}/2) \le \eta_{\mathrm{EE}}^*$, $\eta_{\mathrm{EE}}^{\mathrm{U}} = 1/a \ge \eta_{\mathrm{EE}}^*$, and error tolerance $\epsilon_0>0$, $\epsilon_1>0$, and $\epsilon_2>0$.

Step 2: Let $\eta_{\mathrm{EE}} = \left(\eta_{\mathrm{EE}}^{\mathrm{L}}+\eta_{\mathrm{EE}}^{\mathrm{U}}\right)/2$

{

Let $\boldsymbol{\lambda}^0 = \mathbf{0}$, $\mu_k^0 = -\frac{\theta_k\delta_k\xi_k\left(\eta_{\mathrm{EE}}^{-1}-a+\lambda_k\right)}{2u_k}$ $(k\in\mathcal{K})$ and $t=0$.

Do

{$t\leftarrow t+1$;

Calculate $r_k^t(\lambda_k^t,\mu_k^t)$ and $\beta_k^t(\lambda_k^t,\mu_k^t)$ using (100) and (101);

Calculate $\lambda_k^t\left(r_k^{t-1},\beta_k^{t-1}\right)$ and $\mu_k^t\left(r_k^{t-1},\beta_k^{t-1}\right)$ using (104) and (105).}

While $\left|\beta_k^t-\beta_k^{t-1}\right| > \epsilon_1$ or $\left|r_k^t-r_k^{t-1}\right| > \epsilon_2$

}

Calculate $\eta_{\mathrm{EE}}(\mathbf{r},\boldsymbol{\beta})$ and $J(\mathbf{r},\boldsymbol{\beta},\eta_{\mathrm{EE}})$ using (92) and (97);

If $J(\mathbf{r},\boldsymbol{\beta},\eta_{\mathrm{EE}})>0$, then $\eta_{\mathrm{EE}}^{\mathrm{U}} = \eta_{\mathrm{EE}}(\mathbf{r},\boldsymbol{\beta})$;

Else $\eta_{\mathrm{EE}}^{\mathrm{L}} = \eta_{\mathrm{EE}}(\mathbf{r},\boldsymbol{\beta})$.

Step 3: If $\eta_{\mathrm{EE}}^{\mathrm{U}}-\eta_{\mathrm{EE}}^{\mathrm{L}} < \epsilon_0$, let $\eta_{\mathrm{EE}}^* = \left(\eta_{\mathrm{EE}}^{\mathrm{L}}+\eta_{\mathrm{EE}}^{\mathrm{U}}\right)/2$;

Else go to Step 2.

Step 4: Calculate p and α_k $(k\in\mathcal{K})$ using (90) and (91), respectively.

According to (98) and *Theorem 5*, the optimal power allocation proportions and time switching factors can be obtained by Algorithm 3, which contains two nested loops. The outer loop performs bi-section search for the optimal EE and the inner loop calculates the time switching factors and transmission rates for a given EE value. Once the optimal EE, time switching factors and transmission rates are obtained, we can calculate the optimal transmit power and power allocation proportions using (90) and (91), respectively. Moreover, similar to the initialization setup of Algorithm 1, we set $\eta_{\mathrm{EE}}^{\mathrm{U}} = 1/a \ge \eta_{\mathrm{EE}}^*$ and $\eta_{\mathrm{EE}}^{\mathrm{L}} = \eta_{\mathrm{EE}}\left(\bar{\mathbf{r}},\mathbf{1}/2\right) \le \eta_{\mathrm{EE}}^*$ for the outer loop. For the inner loop, based on (104), initializing $\boldsymbol{\lambda}=\mathbf{0}$ can stop the iteration of $\boldsymbol{\lambda}$ when $\mathbf{r}=\bar{\mathbf{r}}$ is the optimal solution and taking into account (112), we set $\mu_k = -\frac{\theta_k\delta_k\xi_k\left(\eta_{\mathrm{EE}}^{-1}-a+\lambda_k\right)}{2u_k}$ $(k\in\mathcal{K})$.

3) Reference EE: Compared with Algorithm 3, the EE in (92) with the fixed transmission rate $r_k=\bar{r}_k$ $(k\in\mathcal{K})$ is given here based on (89). Since

$$\frac{\mathrm{d}g_k(\bar{r}_k,\beta_k)}{\mathrm{d}\beta_k} = \frac{\sigma_k^2}{\theta_k\delta_k}\left\{\left[\frac{\beta_k\bar{r}_k\ln 2}{B(1-\beta_k)^2}+1\right]\mathrm{e}^{\frac{\bar{r}_k\ln 2}{B(1-\beta_k)}}-1\right\} > 0, \quad k\in\mathcal{K}, \tag{115}$$

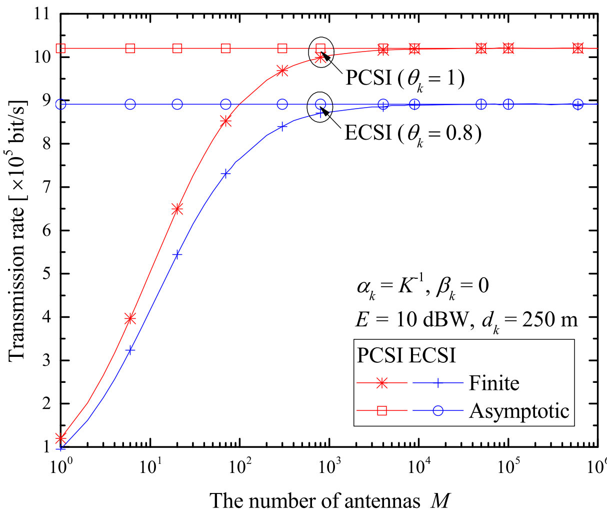

(a) Transmission rate performance.

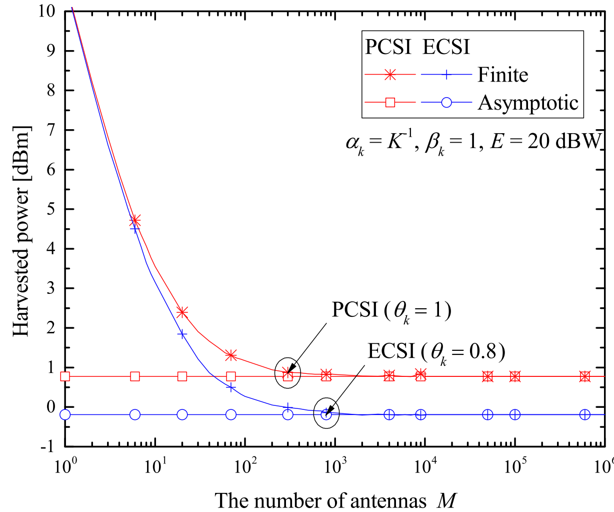

(b) Energy harvesting performance.

Fig. 2. Transmission rate and energy harvesting performance with equal power allocation.

$g_k(\bar{r}_k, \beta_k)$ is monotonically increasing with respect to β_k. Then, applying the bi-section search based on (89), we can obtain the time switching factors $\beta_k\,(k \in \mathcal{K})$ and further calculate the system EE using (92).

V. Simulation Results

This section first evaluates the transmission rate and energy harvesting performance of the massive MIMO system with equal power allocation at the BS. Then, we compare the max-min transmission rate of the power splitting mode with that of the time switching mode under the optimal power allocation proportions and power splitting (or time switching) factors. Then, the EE results are evaluated for both power splitting and time switching modes.

A. Simulation Setup

In the simulations, the default parameters are given as follows. The number of antennas at the BS is $M = 1000$, the number of receivers is $K = 10$, and the system bandwidth is $B = 100$ kHz. All receivers are uniformly distributed on a disc with the inner radius $r = 1$ m and the outer radius $R = 15$ m. The large-scale fading coefficients are $\delta_k = 10^{-3}{d_k}^{-3}\zeta_k$ $(k \in \mathcal{K})$, where d_k represents the distance between the BS and the kth receiver, and ζ_k denotes the log-normal shadow fading, i.e., $10\log_{10}\zeta_k \sim \mathbb{N}\left(0, \sigma_{\text{SF}}^2\right)$ with $\sigma_{\text{SF}} = 8$ dB. The noise power $\sigma_k^2 = BN_k$ $(k \in \mathcal{K})$, where the noise power spectral density $N_k = -120$ dBm/Hz $(k \in \mathcal{K})$.

At the BS, the power efficiency of PAs is $\varsigma = 0.28$, the coefficients of circuit power consumption model are $a = 3.5 \times 10^{-10}$ W/bit, $[b_0, b_1] = \left[1, 2.6 \times 10^{-8}\right]$ W and $c = 20$ W. At the receivers, the energy conversion efficiency is $\xi_k = 0.5$ $(k \in \mathcal{K})$ [21], the power consumption coefficients are $u_k = 0.8 \times 10^{-9}$ W/bit and $v_k = 1$ mW $(k \in \mathcal{K})$ [1], [20], [21]. In the following figures, all results are the average of 10^6 realizations of user distribution on the disc. "PCSI" and "ECSI" represent the results with perfect channel state information (CSI) $(\theta_k = 1, k \in \mathcal{K})$ and estimated CSI $(\theta_k = 0.8, k \in \mathcal{K})$, respectively.

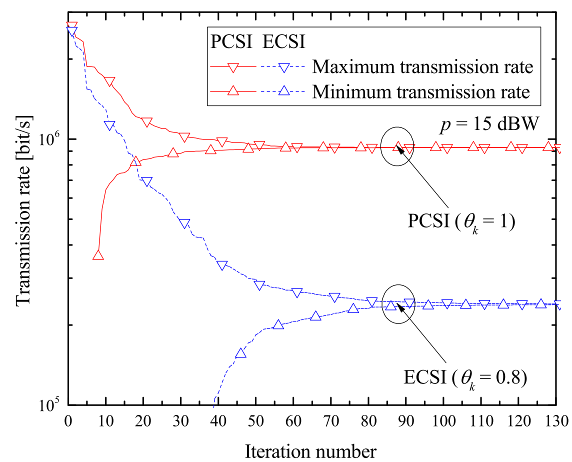

Fig. 3. Transmission rate versus the number of iterations for Algorithm 2.

B. Asymptotic Transmission Rate and Energy Harvesting Performance

In order to verify the asymptotic transmission rate in (12) and harvested power in (7), Fig. 2 illustrates the total transmission rate and harvested power versus the number of antennas with equal power allocation among the receivers, respectively. The transmission rate and harvested power in (6) with the finite number of antennas are computed based on (10) and (4), respectively. In Fig. 2(a), the received signal is fully used for information decoding, i.e., $\beta_k = 0$ $(k \in \mathcal{K})$, therefore the power splitting and time switching modes have the same transmission rate based on (12). With the increasing number of antennas, the transmission rate with the finite number of antennas increases and eventually converges to the asymptotic transmission rate for both perfect CSI and estimated CSI.

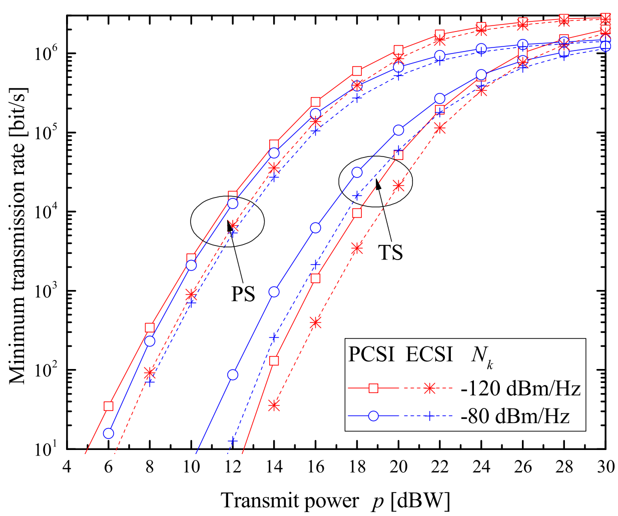

(a) Transmission rate versus the transmit power.

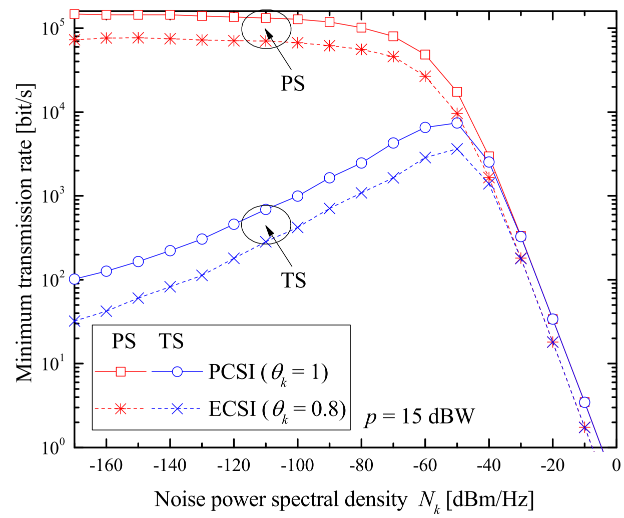

(b) Transmission rate versus the noise power spectral density.

Fig. 4. Transmission rate comparison between power splitting and time switching.

In Fig. 2(b), the received signals are fully used for energy harvesting, i.e., $\beta_k = 1$ $(k \in \mathcal{K})$. For both perfect CSI and estimated CSI, the harvested power with the finite number of antennas decreases with the increasing number of antennas and finally tends to the asymptotic harvested power.

C. Transmission Rate Results

With one-time realization of the channels, Fig. 3 plots the transmission rate of time switching mode versus the number of iterations with $p = 15$ dBW and $\Delta^0 = (1 - \sum_{k=1}^{K} \tilde{\alpha}_k)/(2K)$ for Algorithm 2. When the number of iterations increases, the maximum transmission rate decreases and the minimum transmission rate increases among all receivers, eventually converging to a constant, which demonstrates the convergence of the proposed iterative algorithm for both perfect CSI $(\theta_k = 1, k \in \mathcal{K})$ and estimated CSI $(\theta_k = 0.8, k \in \mathcal{K})$.

The harvested power and transmission rate are respectively determined by the received power and SINR, therefore the minimum transmission rate versus the transmit power p and the noise power spectral density N_k are shown in Figs. 4(a) and 4(b), respectively. The minimum transmission rates of power splitting and time switching modes are calculated by (42) and Algorithm 2 with $\epsilon = 10^{-6}$, respectively. Both Figs. 4(a) and 4(b) indicate that the minimum transmission rate of perfect CSI outperforms that of estimated CSI due to the more accurate MF beamformer of the perfect CSI case; and the power splitting mode performs better than the time switching mode. Fig. 4(a) shows that the minimum transmission rate increases with the increasing transmit power at the BS; and the transmission rate gap between the power splitting mode and time switching mode decreases and eventually becomes zero. With the increasing noise power spectral density, Fig. 4(b) indicates that the minimum transmission rate under the power splitting mode decreases; however it first increases and then decreases under the time switching mode, which satisfies the relationship between the transmission rate and the noise power in (76).

D. Energy Efficiency Results

In order to simplify the EE simulation, we assume that all receivers have the same transmission rate requirements, i.e., $\bar{r}_k = \bar{r}\,(k \in \mathcal{K})$, and the same large-scale fading coefficients, i.e., $\delta_k = 10^{-3} \times d_k^{-3}$ with $d_k = 10$ m $(k \in \mathcal{K})$.

With the required transmission rate $\bar{r} = 10^6$ bit/s $(k \in \mathcal{K})$, Fig. 5(a) illustrates the system EE versus the number of iterations for power splitting mode. In Fig. 5(a), $\eta_{\mathrm{EE}}^{\mathrm{L}}$, $\eta_{\mathrm{EE}}^{\mathrm{U}}$ and η_{EE} represent the lower bound, upper bound and the obtained EE of each iteration in Algorithm 1. With the increasing number of iterations, the upper bound decreases and the lower bound increases, and they rapidly converge to a constant, which verifies the convergence of Algorithm 1 under both perfect CSI and estimated CSI. Moreover, the convergence behavior of the outer iteration of Algorithm 3 is similar to that of Algorithm 1. For the inner iteration of Algorithm 3 with $\bar{r} = 10^6$ bit/s, Fig. 5(b) illustrates the time switching factor and transmission rate versus the number of inner iterations for the first outer iteration. Within a few iterations, the time switching factor β_k and transmission rate r_k rapidly converge for both perfect CSI and estimated CSI. The other variables, i.e., λ_k and μ_k, have the similar convergence behavior.

Fig. 6 depicts the system EE and required transmit power versus the transmission rate requirements for both power splitting and time switching modes. The EEs η_{EE} under power splitting and time switching modes are calculated respectively by (62) with $r_k = \bar{r}_k\,(k \in \mathcal{K})$ and the bisection search in Section IV-B.3; while the optimal EEs η_{EE}^* under power splitting and time switching modes are computed respectively by Algorithms 1 and 3 with $\epsilon = \epsilon_0 = 10^{-8}$ and $\epsilon_1 = \epsilon_2 = 10^{-10}$. The corresponding transmit power values under power splitting and time switching modes are

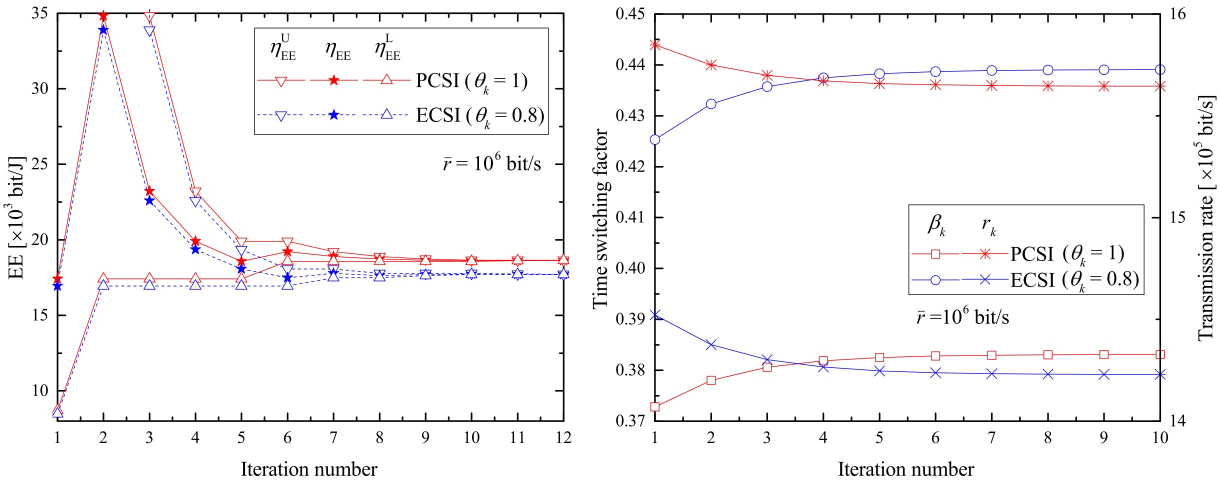

(a) EE versus iteration number in Algorithm 1.

(b) Time switching factor versus iteration number in Algorithm 3.

Fig. 5. Convergence of Algorithms 1 and 3.

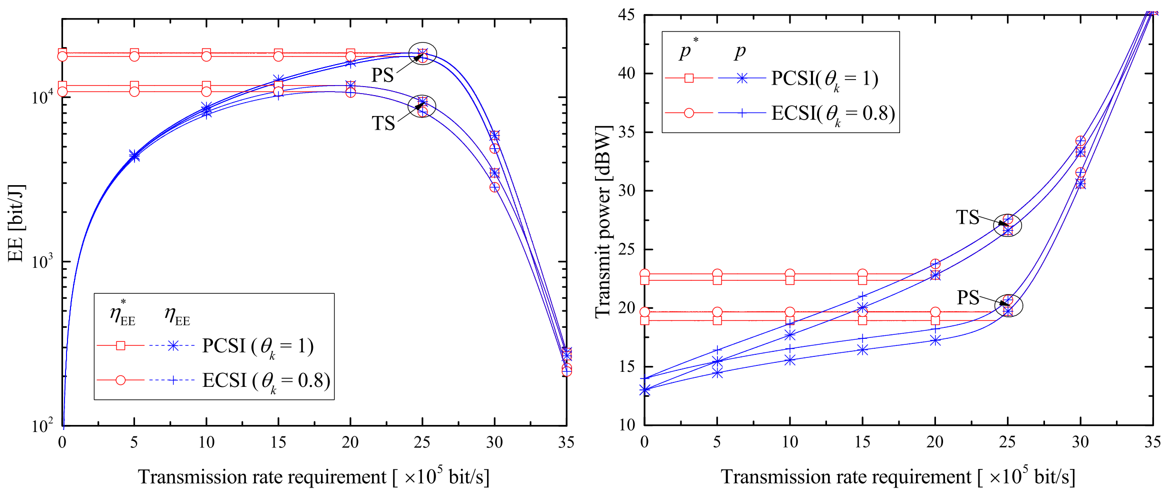

(a) EE versus the transmission rate requirement.

(b) Transmit power versus the transmission rate requirement.

Fig. 6. EE or transmit power comparison between power splitting and time switching.

calculated by (59) and (90), respectively. With the increasing transmission rate requirements of receivers in Fig. 6(a), $\eta_{\rm EE}$ first increases and then decreases; however, $\eta_{\rm EE}^*$ first keeps a constant and then decreases after the maximum value of $\eta_{\rm EE}$. Taking into account Fig. 6(b), the proposed algorithm can adaptively adjust the transmit power in order to satisfy the optimal EE requirement. Moreover, the EE and required transmit power of power splitting mode perform better than those of time switching mode due to the better transmission rate performance of power splitting mode. Further, the EE and required transmit power of perfect CSI outperform those of estimated CSI because the transmission rate of perfect CSI is higher than that of estimated CSI.

VI. Conclusions

Taking into account the circuit power consumption of both BS and the receivers, this paper studied the downlink wireless information and energy transfer in massive MIMO systems. Both the minimum transmission rate among all receivers and the system EE are respectively optimized by jointly designing the power allocation proportions at the BS and the power splitting (or time switching) factors at the power splitting (or time switching) receivers. For the max-min transmission rate problem, the optimal closed-form expression and algorithm are proposed for the power splitting and time switching modes, respectively. For the EE optimization problem, two iterative algorithms are given in order to optimize the system EE for the power splitting and time switching modes. Results indicate that both the transmission rate and EE under the power splitting mode outperform those under the time switching mode.

References

[1] K. Huang and X. Zhou, "Cutting last wires for mobile communication by microwave power transfer," *IEEE Commun. Mag.*, vol. 53, no. 6, pp. 86–93, Jun. 2015.

[2] X. Lu, P. Wang, D. Niyato, D. I. Kim, and Z. Han, "Wireless charging technologies: Fundamentals, standards, and network applications," *IEEE Commun. Surveys Tuts.*, vol. 18, no. 2, pp. 1413–1452, 2nd Quart., 2016.

[3] A. Massa, G. Oliveri, F. Viani, and P. Rocca, "Array designs for long-distance wireless power transmission: State-of-the-art and innovative solutions," *Proc. IEEE*, vol. 101, no. 6, pp. 1464–1481, Jun. 2013.

[4] I. Krikidis, S. Timotheou, S. Nikolaou, G. Zheng, D. W. K. Ng, and R. Schober, "Simultaneous wireless information and power transfer in modern communication systems," *IEEE Commun. Mag.*, vol. 52, no. 11, pp. 104–110, Nov. 2014.

[5] J. Park, B. Clerckx, C. Song, and Y. Wu, "An analysis of the optimum node density for simultaneous wireless information and power transfer in Ad hoc networks," *IEEE Trans. Veh. Technol.*, vol. 67, no. 3, pp. 2713–2726, Mar. 2018.

[6] B. Clerckx, "Wireless information and power transfer: Nonlinearity, waveform design and rate-energy tradeoff," *IEEE Trans. Signal Process.*, vol. 66, no. 4, pp. 847–862, Feb. 2018.

[7] B. Clerckx, R. Zhang, R. Schober, D. W. K. Ng, D. I. Kim, and H. V. Poor, "Fundamentals of wireless information and power transfer: From RF energy harvester models to signal and system designs," *IEEE J. Sel. Areas Commun.*, vol. 37, no. 1, pp. 4–33, Jan. 2018.

[8] R. Zhang and C. K. Ho, "MIMO broadcasting for simultaneous wireless information and power transfer," *IEEE Trans. Wireless Commun.*, vol. 12, no. 5, pp. 1989–2001, May 2013.

[9] T. L. Marzetta, "Noncooperative cellular wireless with unlimited numbers of base station antennas," *IEEE Trans. Wireless Commun.*, vol. 9, no. 11, pp. 3590–3600, Nov. 2010.

[10] K. Zheng, L. Zhao, J. Mei, B. Shao, W. Xiang, and L. Hanzo, "Survey of large-scale MIMO systems," *IEEE Commun. Surveys Tuts.*, vol. 17, no. 3, pp. 1738–1760, 3rd Quart., 2015.

[11] G. Yang, C. K. Ho, R. Zhang, and Y. L. Guan, "Throughput optimization for massive MIMO systems powered by wireless energy transfer," *IEEE J. Sel. Areas Commun.*, vol. 33, no. 8, pp. 1640–1650, Aug. 2015.

[12] L. Zhao, X. Wang, and K. Zheng, "Downlink hybrid information and energy transfer with massive MIMO," *IEEE Trans. Wireless Commun.*, vol. 15, no. 2, pp. 1309–1322, Feb. 2016.

[13] S. Kashyap, E. Björnson, and E. G. Larsson, "On the feasibility of wireless energy transfer using massive antenna arrays," *IEEE Trans. Wireless Commun.*, vol. 15, no. 5, pp. 3466–3480, May 2016.

[14] S. Lee, Y. Zeng, and R. Zhang, "Retrodirective multi-user wireless power transfer with massive MIMO," *IEEE Wireless Commun. Lett.*, vol. 7, no. 1, pp. 54–57, Feb. 2018.

[15] G. Amarasuriya, E. G. Larsson, and H. V. Poor, "Wireless information and power transfer in multiway massive MIMO relay networks," *IEEE Trans. Wireless Commun.*, vol. 15, no. 6, pp. 3837–3855, Jun. 2016.

[16] L. Zhao, X. Wang, and T. Riihonen, "Transmission rate optimization of full-duplex relay systems powered by wireless energy transfer," *IEEE Trans. Wireless Commun.*, vol. 16, no. 10, pp. 6438–6450, Oct. 2017.

[17] H. H. M. Tam, H. D. Tuan, A. A. Nasir, T. Q. Duong, and H. V. Poor, "MIMO energy harvesting in full-duplex multi-user networks," *IEEE Trans. Wireless Commun.*, vol. 16, no. 5, pp. 3282–3297, May 2017.

[18] X. Zhou, R. Zhang, and C. K. Ho, "Wireless information and power transfer: Architecture design and rate-energy tradeoff," *IEEE Trans. Commun.*, vol. 61, no. 11, pp. 4754–4767, Nov. 2013.

[19] Z. Ni and M. Motani, "Performance of energy-harvesting receivers with time-switching architecture," *IEEE Trans. Wireless Commun.*, vol. 16, no. 11, pp. 7252–7263, Nov. 2017.

[20] E. Björnson, L. Sanguinetti, J. Hoydis, and M. Debbah, "Optimal design of energy-efficient multi-user MIMO systems: Is massive MIMO the answer?" *IEEE Trans. Wireless Commun.*, vol. 14, no. 6, pp. 3059–3075, Oct. 2015.

[21] L. Zhao and X. Wang, "Round-trip energy efficiency of wireless energy powered massive MIMO system with latency constraint," *IEEE Commun. Lett.*, vol. 21, no. 1, pp. 12–15, Jan. 2017.

[22] T. A. Khan, A. Yazdan, and R. W. Heath, Jr., "Optimization of power transfer efficiency and energy efficiency for wireless-powered systems with massive MIMO," *IEEE Trans. Wireless Commun.*, vol. 17, no. 11, pp. 7159–7172, Nov. 2018.

[23] H. Q. Ngo, E. G. Larsson, and T. L. Marzetta, "Aspects of favorable propagation in massive MIMO," in *Proc. 22nd Eur. Signal Process. Conf. (EUSIPCO)*, Lisbon, Portugal, Sep. 2014, pp. 76–80.

[24] W. Xu, J. Liu, S. Jin, and X. Dong, "Spectral and energy efficiency of multi-pair massive MIMO relay network with hybrid processing," *IEEE Trans. Commun.*, vol. 65, no. 9, pp. 3794–3808, Sep. 2017.

[25] H. Q. Ngo, E. G. Larsson, and T. L. Marzetta, "Energy and spectral efficiency of very large multiuser MIMO systems," *IEEE Trans. Commun.*, vol. 61, no. 4, pp. 1436–1449, Apr. 2013.

[26] H. Chen, Y. Li, Y. Jiang, Y. Ma, and B. Vucetic, "Distributed power splitting for SWIPT in relay interference channels using game theory," *IEEE Trans. Wireless Commun.*, vol. 14, no. 1, pp. 410–420, Jan. 2015.

[27] Y. Li, B. Bakkaloglu, and C. Chakrabarti, "A system level energy model and energy-quality evaluation for integrated transceiver front-ends," *IEEE Trans. Very Large Scale Integr. (VLSI) Syst.*, vol. 15, no. 1, pp. 90–103, Jan. 2007.

[28] W. Rhee, *Wireless Transceiver Circuits: System Perspectives and Design Aspects (Device, Circuit, and Systems)*, Boca Raton, FL, USA: CRC Press, 2015.

[29] Z. Zhang, J. Chen, and J. Hu, "Energy-efficiency massive MIMO system analysis: From a circuit power perspective," in *Proc. IEEE Int. Conf. Digit. Signal Process. (DSP)*, Beijing, China, Oct. 2016, pp. 350–354.

[30] E. Björnson, M. Matthaiou, and M. Debbah, "Massive MIMO with non-idea arbitrary arrays: Hardware scaling laws and circuit-aware design," *IEEE Trans. Wireless Commun.*, vol. 14, no. 8, pp. 4353–4368, Aug. 2015.

[31] E. Björnson, J. Hoydis, and L. Sanguinetti, *Massive MIMO Networks: Spectral, Energy, and Hardware Efficiency*. Hanover, MA, USA: Now Publishers, 2017.

[32] Y. Xin, D. Wang, J. Li, H. Zhu, J. Wang, and X. You, "Area spectral efficiency and area energy efficiency of massive MIMO cellular systems," *IEEE Trans. Veh. Technol.*, vol. 65, no. 5, pp. 3243–3253, May 2016.

[33] Z. Xu, C. Yang, G. Y. Li, Y. Chen, S. Zhang, and S. Xu, "Energy-efficient configuration of spatial and frequency resources in MIMO-OFDMA systems," *IEEE Trans. Commun.*, vol. 61, no. 2, pp. 564–575, Feb. 2013.

[34] R. M. Corless, G. H. Gonnet, D. E. G. Hare, D. J. Jeffrey, and D. E. Knuth, "On the Lambert W function," *Adv. Comput. Math.*, vol. 5, no. 1, pp. 329–359, 1996.

[35] S. Boyd and L. Vandenberghe, *Convex Optimization*. Cambridge, U.K.: Cambridge Univ. Press, 2004.

[36] C. Isheden, Z. Chong, E. Jorswieck, and G. Fettweis, "Framework for link-level energy efficiency optimization with informed transmitter," *IEEE Trans. Wireless Commun.*, vol. 11, no. 8, pp. 2946–2957, Aug. 2012.

[37] K. Shen and W. Yu, "Fractional programming for communication systems—Part I: Power control and beamforming," *IEEE Trans. Signal Process.*, vol. 66, no. 10, pp. 2616–2630, May 2018.

[38] H. Zhang, S. Huang, C. Jiang, K. Long, V. C. M. Leung, and H. V. Poor, "Energy efficient user association and power allocation in millimeter-wave-based ultra dense networks with energy harvesting base stations," *IEEE J. Sel. Areas Commun.*, vol. 35, no. 9, pp. 1936–1947, Sep. 2017.

Long Zhao (M'17) received the Ph.D. degree from the Beijing University of Posts and Telecommunications (BUPT), Beijing, China, in 2015. From 2014 to 2015, he was a Visiting Scholar at the Department of Electrical Engineering, Columbia University, New York, NY, USA. He is currently an Associate Professor with BUPT. His research interests include wireless communications and signal processing.

Xiaodong Wang (S'98–M'98–SM'04–F'08) received the Ph.D. degree in electrical engineering from Princeton University. He is currently a Professor of electrical engineering with Columbia University, New York, NY, USA. His research interests fall in the general areas of computing, signal processing, and communications, and he has published extensively in these areas. He has published a book *Wireless Communication Systems: Advanced Techniques for Signal Reception* (Prentice-Hall, 2003). His current research interests include wireless communications, statistical signal processing, and genomic signal processing. He is listed as an ISI highly-cited author. He was a recipient of the 1999 NSF CAREER Award, the 2001 IEEE Communications Society and Information Theory Society Joint Paper Award, and the 2011 IEEE Communication Society Award for Outstanding Paper on New Communication Topics. He has served as an Associate Editor for the IEEE TRANSACTIONS ON COMMUNICATIONS, the IEEE TRANSACTIONS ON WIRELESS COMMUNICATIONS, the IEEE TRANSACTIONS ON SIGNAL PROCESSING, and the IEEE TRANSACTIONS ON INFORMATION THEORY.